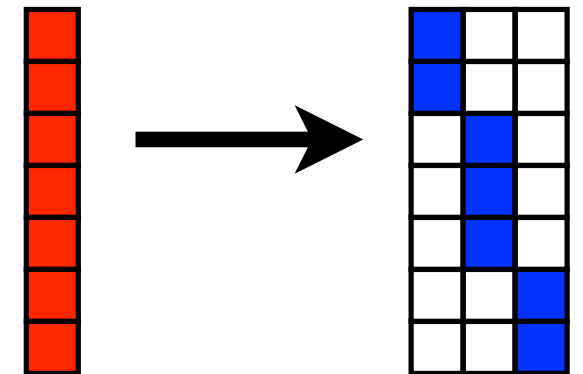
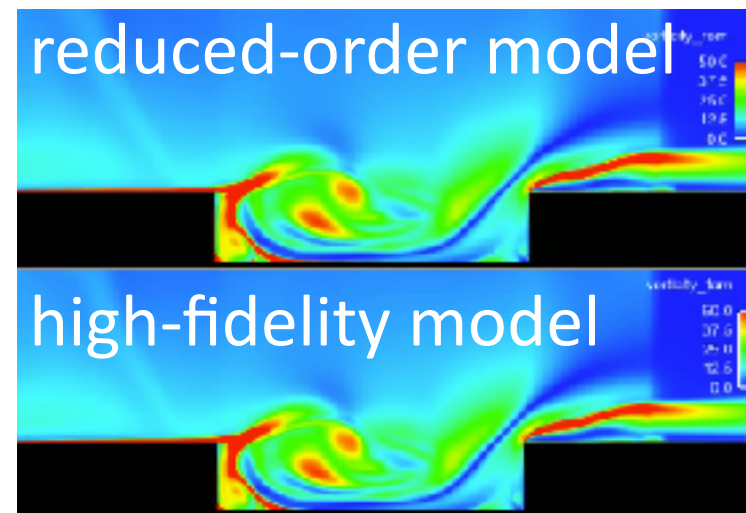
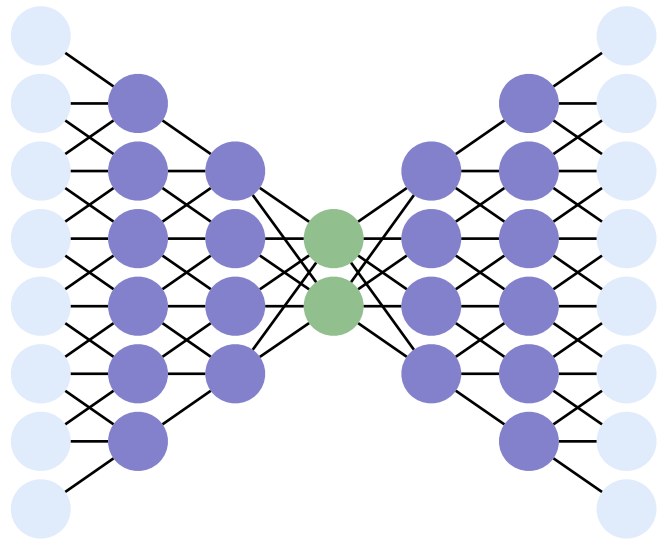


# Convolutional autoencoders and LSTMs

Using deep learning to overcome Kolmogorov-width limitations and accurately model errors in nonlinear model reduction



*Kookjin Lee*



*Eric Parish*

**Kevin Carlberg**

University of Washington

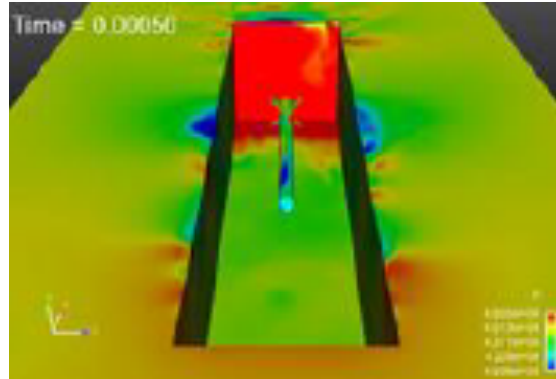
*Mathematics of Reduced-Order Models*

ICERM, Providence, Rhode Island

February 21, 2020

# High-fidelity simulation

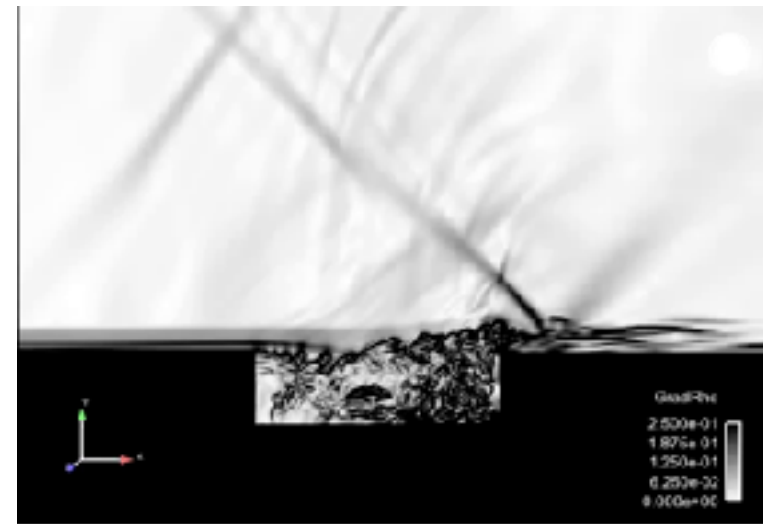
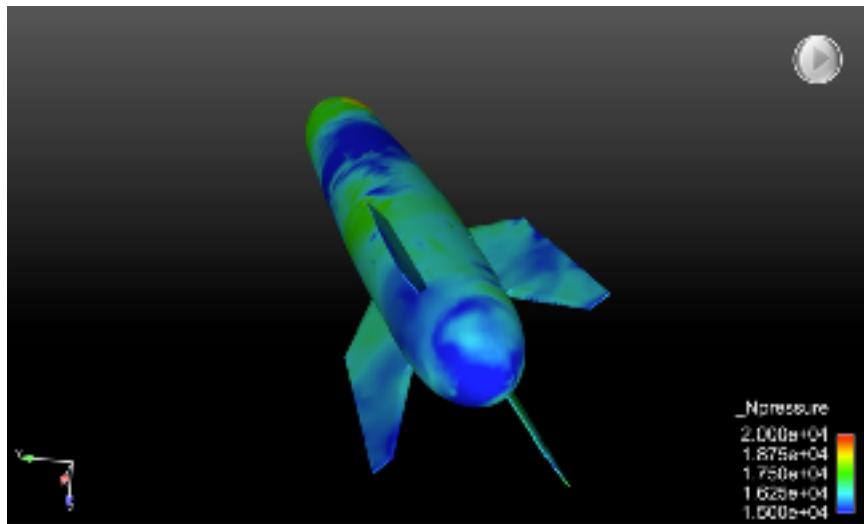
- + **Indispensable** in science and engineering
- **Extreme-scale** models required for high fidelity





# High-fidelity simulation

- + **Indispensable** in science and engineering
- **Extreme-scale** models required for high fidelity



- + *High fidelity*: matches wind-tunnel experiments to within **5%**
- *Extreme scale*: **100 million cells, 200,000 time steps**
- *High simulation costs*: **6 weeks, 5000 cores**

**computational barrier**

## Many-query problems

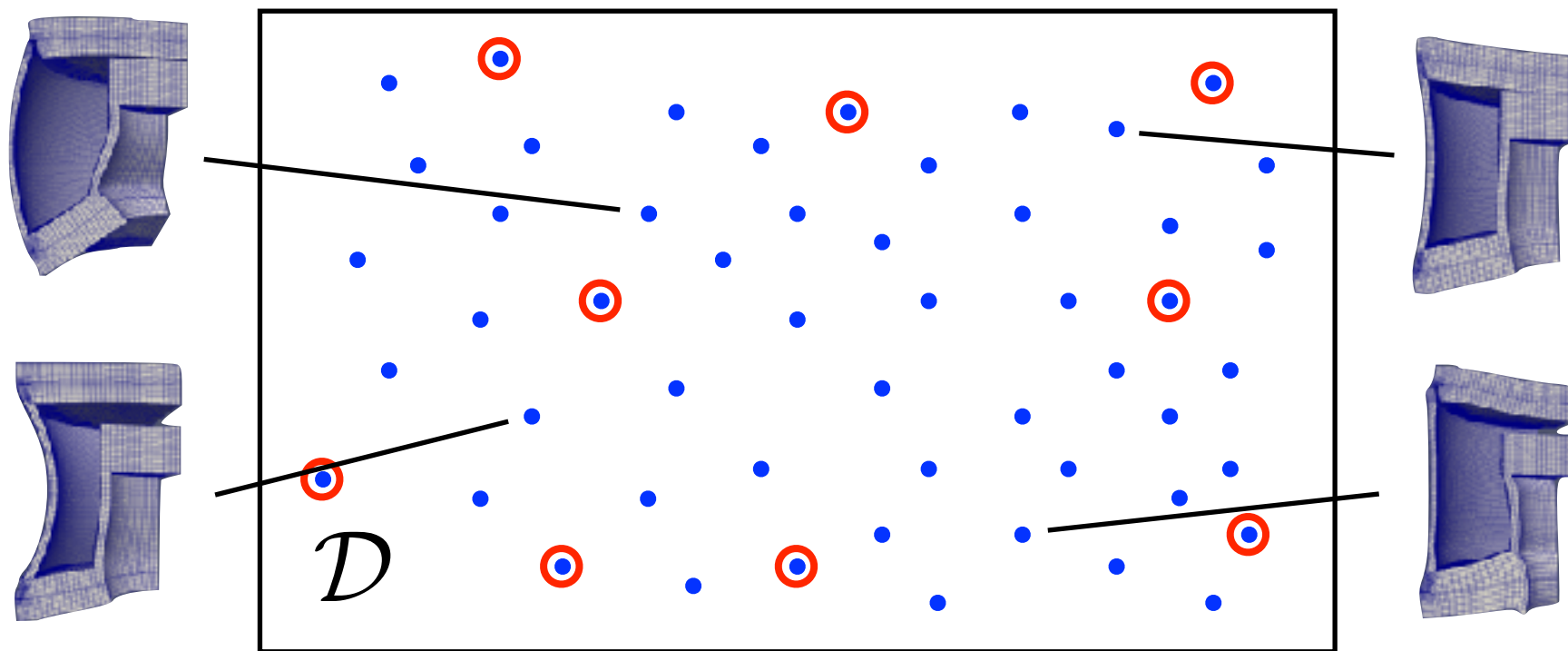
- uncertainty propagation
- Bayesian inference
- stochastic optimization

***Goal: break computational barrier***

# Approach: exploit simulation data

$$\text{ODE: } \frac{d\mathbf{x}}{dt} = \mathbf{f}(\mathbf{x}; t, \mu), \quad \mathbf{x}(0, \mu) = \mathbf{x}_0(\mu), \quad t \in [0, T_{\text{final}}], \quad \mu \in \mathcal{D}$$

*Many-query problem: solve ODE for  $\mu \in \mathcal{D}_{\text{query}}$*

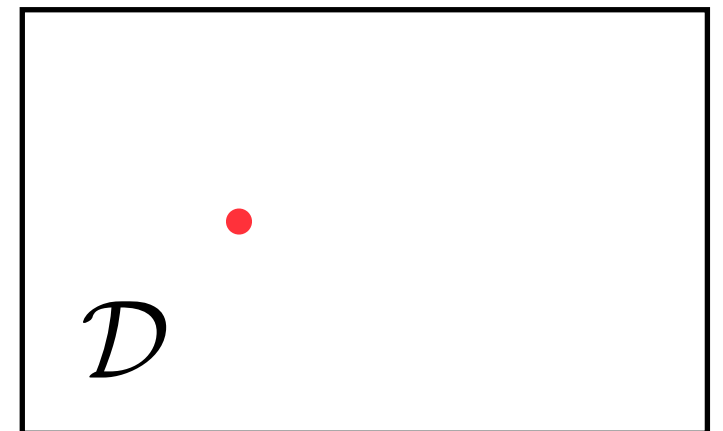
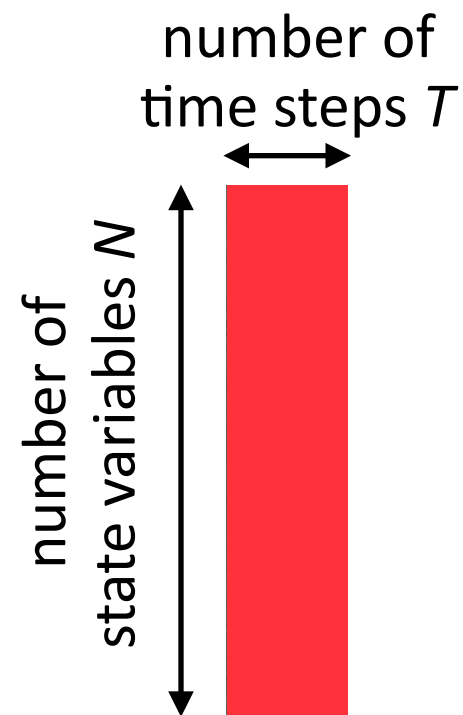
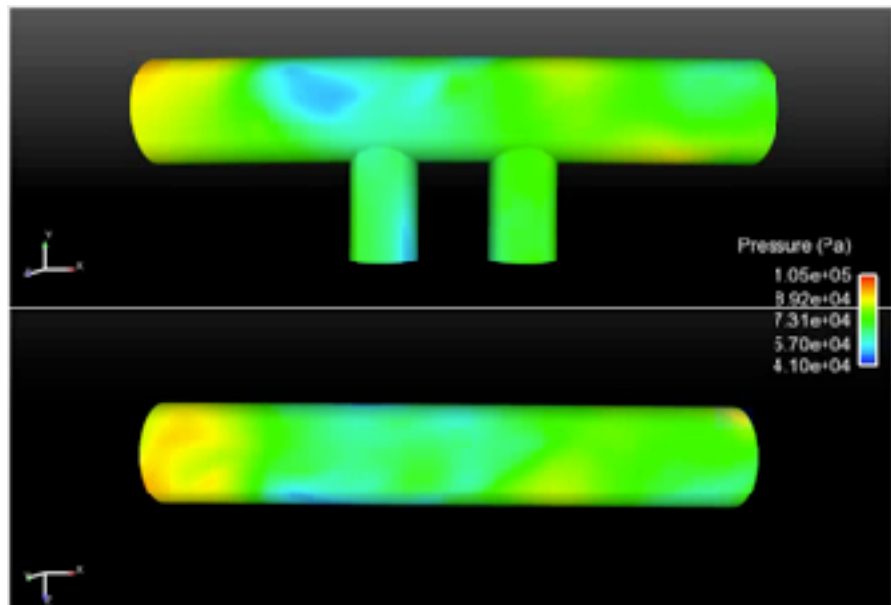


*Idea: exploit simulation data collected at **a few points***



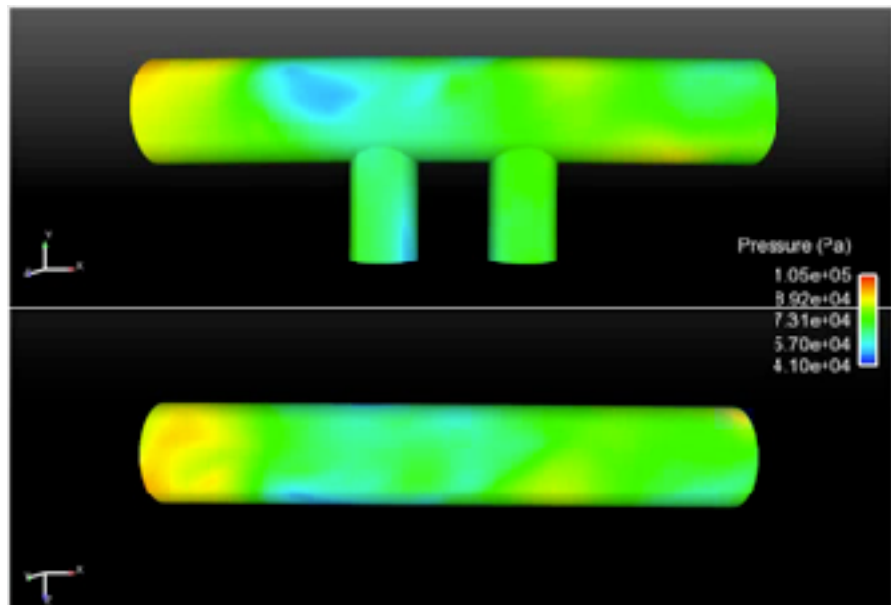
1. *Training*: Solve ODE for  $\mu \in \mathcal{D}_{\text{training}}$  and collect simulation data
2. *Machine learning*: Identify structure in data
3. *Reduction*: Reduce the cost of solving ODE for  $\mu \in \mathcal{D}_{\text{query}} \setminus \mathcal{D}_{\text{training}}$

$$\text{ODE: } \frac{d\mathbf{x}}{dt} = \mathbf{f}(\mathbf{x}; t, \mu)$$

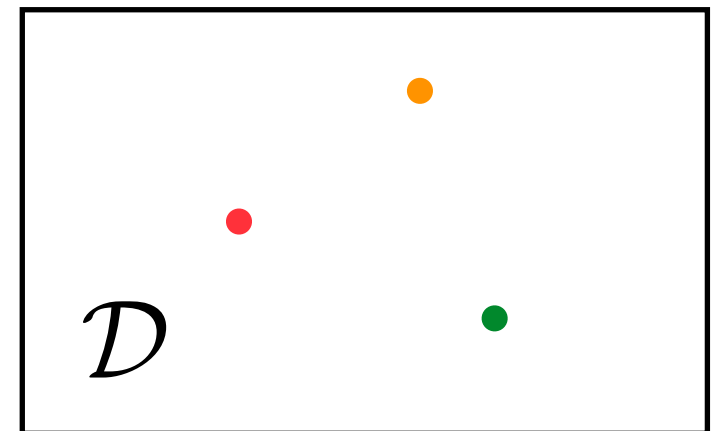
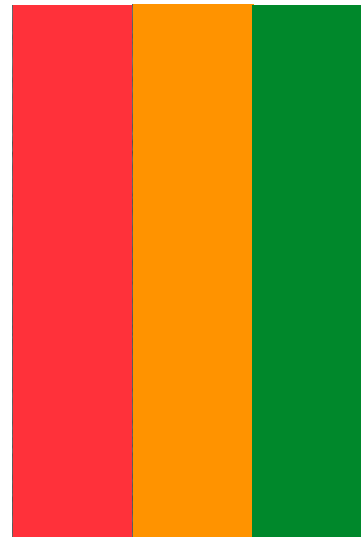


1. *Training*: Solve ODE for  $\mu \in \mathcal{D}_{\text{training}}$  and collect simulation data
2. *Machine learning*: Identify structure in data
3. *Reduction*: Reduce the cost of solving ODE for  $\mu \in \mathcal{D}_{\text{query}} \setminus \mathcal{D}_{\text{training}}$

$$\text{ODE: } \frac{d\mathbf{x}}{dt} = \mathbf{f}(\mathbf{x}; t, \mu)$$



$\mathbf{x} =$





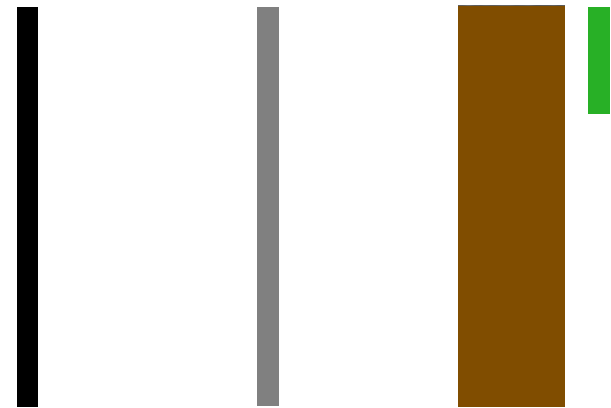
1. *Training*: Solve ODE for  $\mu \in \mathcal{D}_{\text{training}}$  and collect simulation data
2. *Machine learning*: Identify structure in data
3. *Reduction*: Reduce the cost of solving ODE for  $\mu \in \mathcal{D}_{\text{query}} \setminus \mathcal{D}_{\text{training}}$

$$\mathbf{X} = \begin{array}{|c|c|c|} \hline \text{red} & \text{orange} & \text{green} \\ \hline \end{array} = \begin{array}{|c|c|} \hline \Phi & \mathbf{U} \\ \hline \end{array} \begin{array}{c} \diagdown \\ \Sigma \end{array} \begin{array}{|c|} \hline \mathbf{V}^T \\ \hline \end{array}$$

$\Phi$  columns are principal components of the spatial simulation data

1. *Training*: Solve ODE for  $\mu \in \mathcal{D}_{\text{training}}$  and collect simulation data
2. *Machine learning*: Identify structure in data
3. *Reduction*: Reduce the cost of solving ODE for  $\mu \in \mathcal{D}_{\text{query}} \setminus \mathcal{D}_{\text{training}}$

$$\mathbf{x}(t) \approx \tilde{\mathbf{x}}(t) = \Phi \hat{\mathbf{x}}(t)$$



ODE

$$\frac{d\mathbf{x}}{dt} = \mathbf{f}(\mathbf{x}; t)$$

residual  
minimization

Galerkin ODE

$$\frac{d\hat{\mathbf{x}}}{dt} = \Phi^T \mathbf{f}(\Phi \hat{\mathbf{x}}, t)$$

$$\mathbf{r}\left(\frac{d\mathbf{x}}{dt}, \mathbf{x}, t\right) = \mathbf{0}$$

$$\Phi \frac{d\hat{\mathbf{x}}}{dt}(\Phi \hat{\mathbf{x}}, t) = \arg \min_{\mathbf{v} \in \text{range}(\Phi)} \|\mathbf{r}(\mathbf{v}, \Phi \hat{\mathbf{x}}, t)\|_2$$

time  
discretization

OΔE

$$\mathbf{r}^n(\mathbf{x}^n) = \mathbf{0}$$

$$n = 1, \dots, T$$

residual  
minimization

LSPG OΔE

[C., Bou-Mosleh, Farhat, 2011]

$$\Phi \hat{\mathbf{x}}^n = \arg \min_{\mathbf{v} \in \text{range}(\Phi)} \|\mathbf{r}^n(\mathbf{v})\|_2$$

$$n = 1, \dots, T$$

time  
discretization

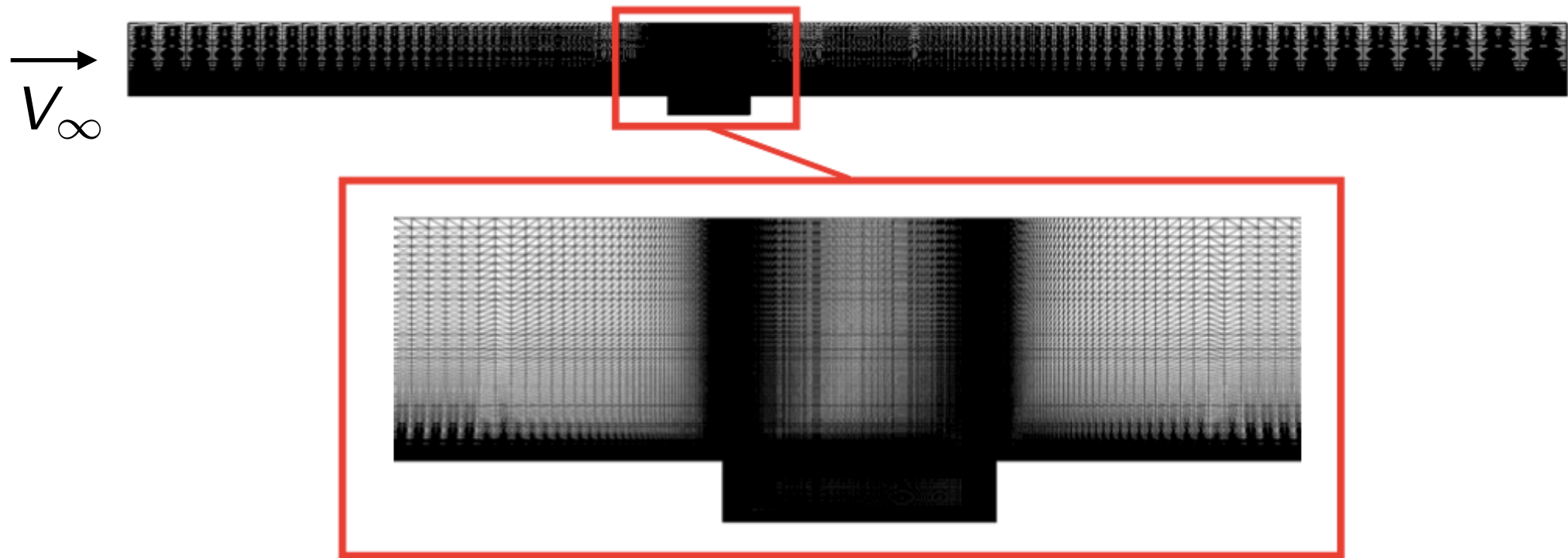
Galerkin OΔE

$$\Phi^T \mathbf{r}^n(\Phi \hat{\mathbf{x}}^n) = \mathbf{0}$$

$$n = 1, \dots, T$$

- ▶ ODE residual:  $\mathbf{r}(\mathbf{v}, \mathbf{x}, t) := \mathbf{v} - \mathbf{f}(\mathbf{x}, t)$
- ▶ OΔE residual:  $\mathbf{r}^n(\mathbf{w}) := \alpha_0 \mathbf{w} - \Delta t \beta_0 \mathbf{f}(\mathbf{w}, t^n) + \sum_{j=1}^k \alpha_j \mathbf{x}^{n-j} - \Delta t \sum_{j=1}^k \beta_j \mathbf{f}(\mathbf{x}^{n-j}, t^{n-j})$
- ▶ Other residual-minimizing ROMs [LeGresley and Alonso, 2000; Bui-Thanh et al., 2008; Bui-Thanh et al., 2008; Constantine and Wang, 2012; Choi and C., 2019; **Parish and C., 2019**]

# Captive carry



- Unsteady Navier–Stokes
- $\text{Re} = 6.3 \times 10^6$
- $M_\infty = 0.6$

## Spatial discretization

- 2nd-order finite volume
- DES turbulence model
- $1.2 \times 10^6$  degrees of freedom

## Temporal discretization

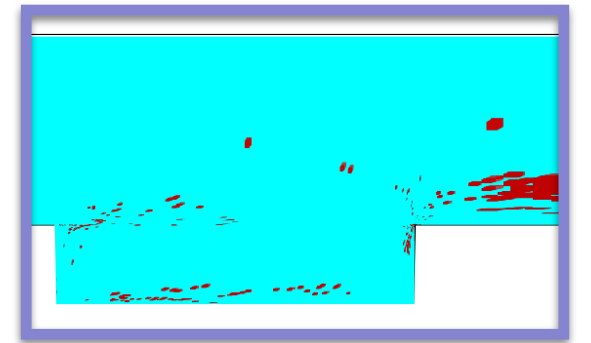
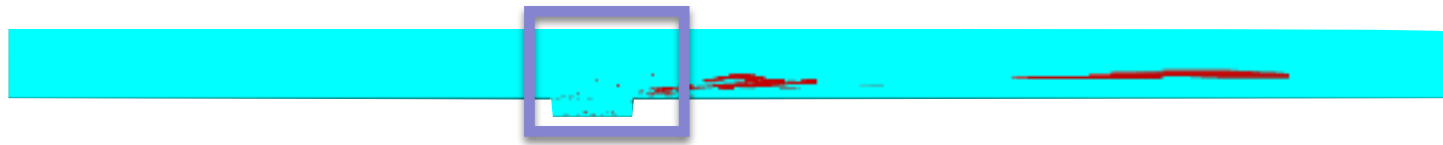
- 2nd-order BDF
- Verified time step  $\Delta t = 1.5 \times 10^{-3}$
- $8.3 \times 10^3$  time instances



# LSPG ROM with sample mesh [C., Farhat, Cortial, Amsallem, 2013]

$$\Phi \hat{\mathbf{x}}^n = \arg \min_{\mathbf{v} \in \text{range}(\Phi)} \|\mathbf{r}^n(\mathbf{v})\|_{\Theta}$$

sample  
mesh



+ *HPC on a laptop*

*vorticity field*

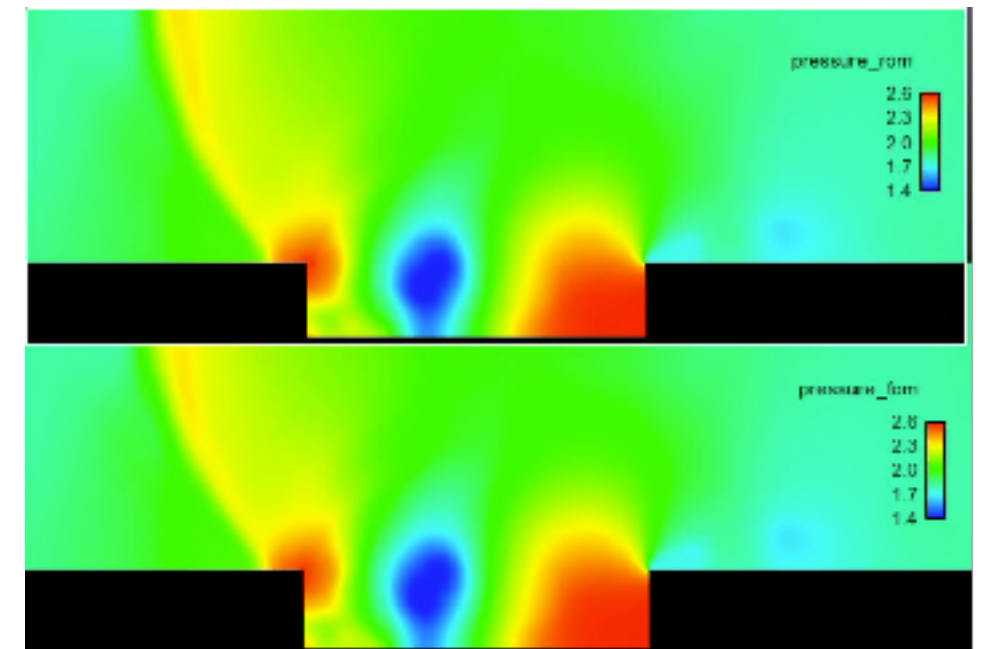
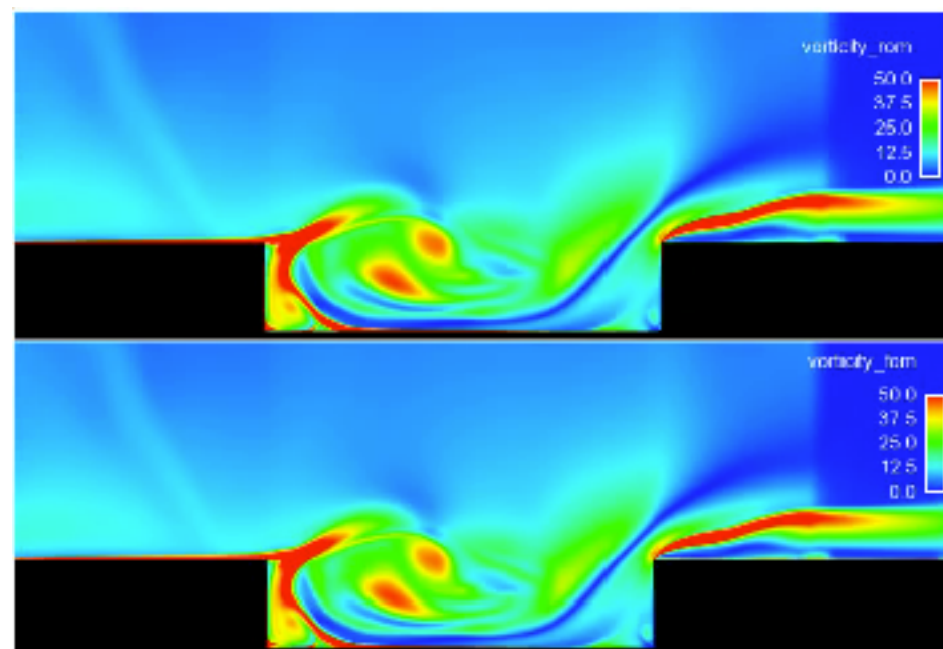
*pressure field*

LSPG ROM

32 min, 2 cores

high-fidelity

5 hours, 48 cores



+ 229x savings in core-hours

+ < 1% error in time-averaged drag

***... so why doesn't everyone use ROMs?***

# Outstanding challenges in model reduction

## 1) Linear-subspace assumption is strong

$$\mathbf{x}(t) \approx \tilde{\mathbf{x}}(t) = \Phi \hat{\mathbf{x}}(t)$$

- Lee and C. “Model reduction of dynamical systems on nonlinear manifolds using deep convolutional autoencoders.” J Comp Phys, 404:108973, 2020.

## 2) Important physical properties not satisfied

$$\Phi \frac{d\hat{\mathbf{x}}}{dt}(\mathbf{x}, t) = \underset{\mathbf{v} \in \text{range}(\Phi)}{\text{argmin}} \|\mathbf{r}(\mathbf{v}, \mathbf{x}; t)\|_2 \quad \text{Galerkin}$$

$$\Phi \hat{\mathbf{x}}^n = \underset{\mathbf{v} \in \text{range}(\Phi)}{\text{argmin}} \|\mathbf{r}^n(\mathbf{v})\|_2 \quad \text{LSPG}$$

- C., Choi, and Sargsyan. “Conservative model reduction for finite-volume models.” J Comp Phys, 371:280–314, 2018.
- Lee and C. “Deep conservation: A latent dynamics model for exact satisfaction of physical conservation laws.” arXiv e-print 1909.09754, 2019.

## 3) Error analysis difficult

- Freno and C. “Machine-learning error models for approximate solutions to parameterized systems of nonlinear equations.” CMAME, 348:250–296, 2019.
- Parish and C. “Time-series machine-learning error models for approximate solutions to parameterized dynamical systems.” arXiv e-print, (1907.11822).

# Outstanding challenges in model reduction

## 1) Linear-subspace assumption is strong

$$\mathbf{x}(t) \approx \tilde{\mathbf{x}}(t) = \Phi \hat{\mathbf{x}}(t)$$

- Lee and C. “Model reduction of dynamical systems on nonlinear manifolds using deep convolutional autoencoders.” J Comp Phys, 404:108973, 2020.

## 2) Important physical properties not guaranteed

<i>Galerkin</i>	<i>LSPG</i>
$\Phi \frac{d\hat{\mathbf{x}}}{dt}(\mathbf{x}, t) = \operatorname{argmin}_{\mathbf{v} \in \operatorname{range}(\Phi)} \ \mathbf{r}(\mathbf{v}, \mathbf{x}; t)\ _2$	$\Phi \hat{\mathbf{x}}^n = \operatorname{argmin}_{\mathbf{v} \in \operatorname{range}(\Phi)} \ \mathbf{r}^n(\mathbf{v})\ _2$

- C., Choi, and Sargsyan. “Conservative model reduction for finite-volume models.” J Comp Phys, 371:280–314, 2018.
- Lee and C. “Deep conservation: A latent dynamics model for exact satisfaction of physical conservation laws.” arXiv e-print 1909.09754, 2019.

## 3) Error analysis difficult

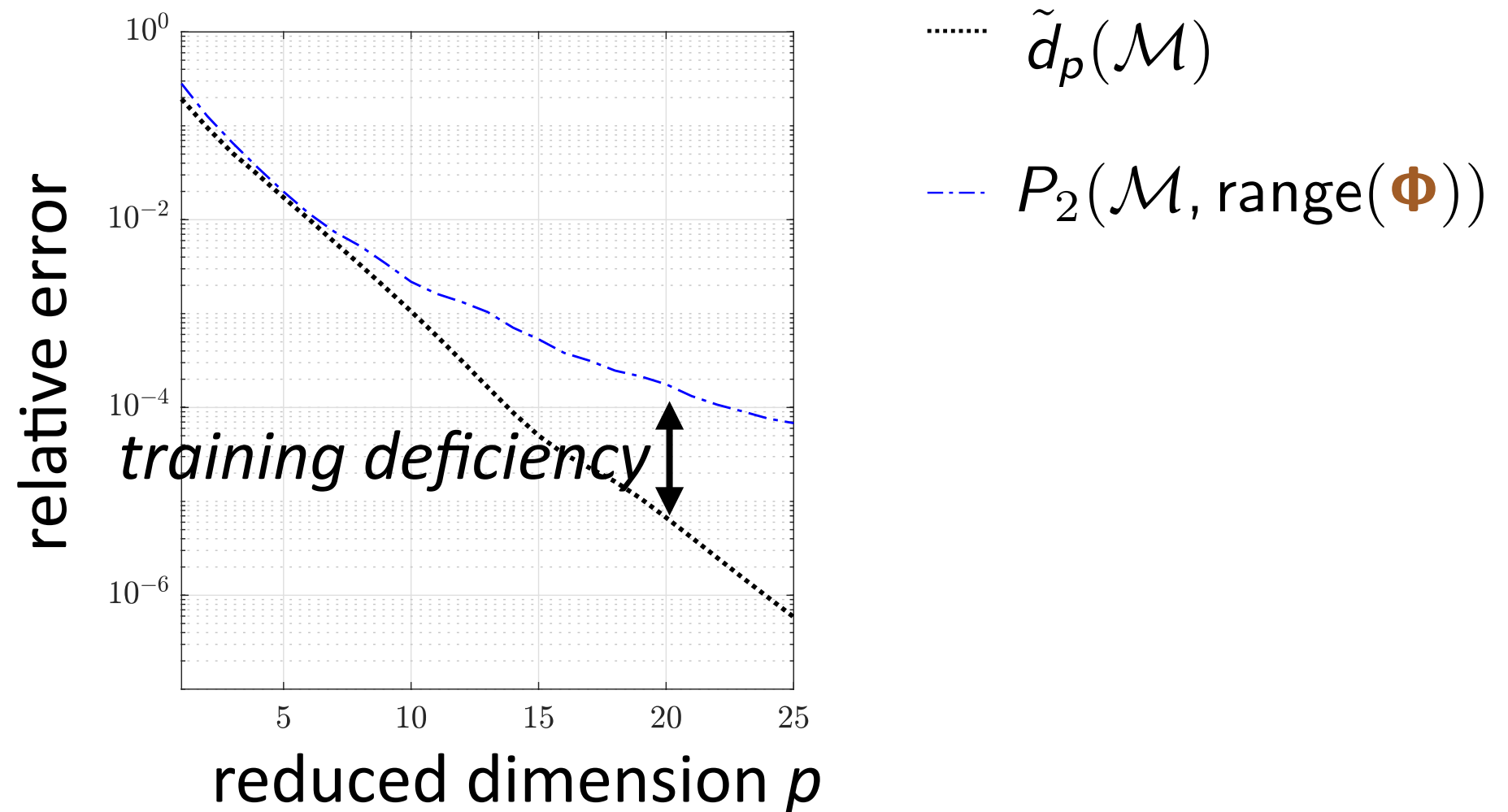
- Freno and C. “Machine-learning error models for approximate solutions to parameterized systems of nonlinear equations.” CMAME, 348:250–296, 2019.
- Parish and C. “Time-series machine-learning error models for approximate solutions to parameterized dynamical systems.” arXiv e-print, (1907.11822).

# Kolmogorov-width limitation of linear subspaces

- $\mathcal{M} := \{\mathbf{x}(t, \boldsymbol{\mu}) \mid t \in [0, T_{\text{final}}], \boldsymbol{\mu} \in \mathcal{D}\}$ : solution manifold
- $\mathcal{S}_p$ : set of all  $p$ -dimensional linear subspaces
- $d_p(\mathcal{M}) := \inf_{\mathcal{S} \in \mathcal{S}_p} P_\infty(\mathcal{M}, \mathcal{S}), P_\infty(\mathcal{M}, \mathcal{S}) := \sup_{\mathbf{x} \in \mathcal{M}} \inf_{\mathbf{y} \in \mathcal{S}} \|\mathbf{x} - \mathbf{y}\|$

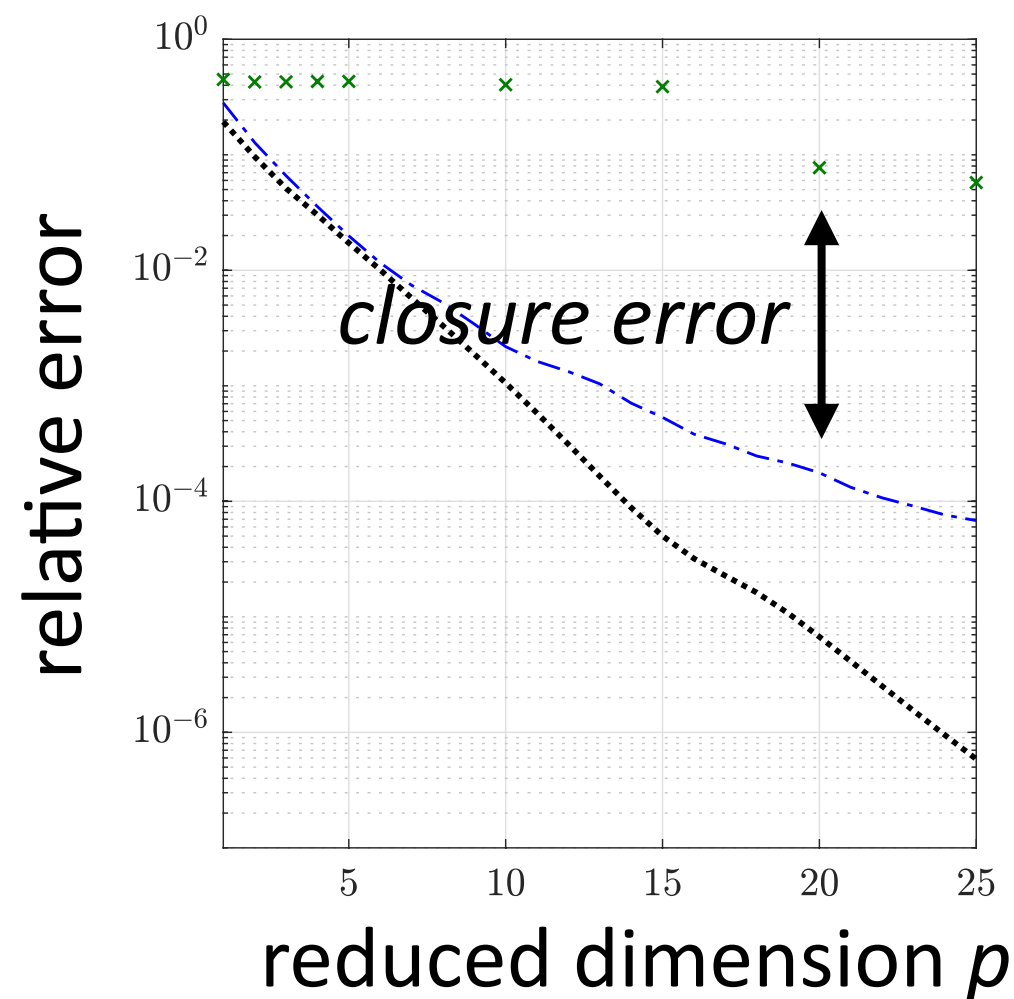
# Kolmogorov-width limitation of linear subspaces

- $\mathcal{M} := \{\mathbf{x}(t, \boldsymbol{\mu}) \mid t \in [0, T_{\text{final}}], \boldsymbol{\mu} \in \mathcal{D}\}$ : solution manifold
- $\mathcal{S}_p$ : set of all  $p$ -dimensional linear subspaces
- $\tilde{d}_p(\mathcal{M}) := \inf_{\mathcal{S} \in \mathcal{S}_p} P_2(\mathcal{M}, \mathcal{S})$ ,  $P_2(\mathcal{M}, \mathcal{S}) := \sqrt{\sum_{\mathbf{x} \in \mathcal{M}} \inf_{\mathbf{y} \in \mathcal{S}} \|\mathbf{x} - \mathbf{y}\|^2} / \sqrt{\sum_{\mathbf{x} \in \mathcal{M}} \|\mathbf{x}\|^2}$



# Kolmogorov-width limitation of linear subspaces

- $\mathcal{M} := \{\mathbf{x}(t, \boldsymbol{\mu}) \mid t \in [0, T_{\text{final}}], \boldsymbol{\mu} \in \mathcal{D}\}$ : solution manifold
- $\mathcal{S}_p$ : set of all  $p$ -dimensional linear subspaces
- $\tilde{d}_p(\mathcal{M}) := \inf_{\mathcal{S} \in \mathcal{S}_p} P_2(\mathcal{M}, \mathcal{S})$ ,  $P_2(\mathcal{M}, \mathcal{S}) := \sqrt{\sum_{\mathbf{x} \in \mathcal{M}} \inf_{\mathbf{y} \in \mathcal{S}} \|\mathbf{x} - \mathbf{y}\|^2} / \sqrt{\sum_{\mathbf{x} \in \mathcal{M}} \|\mathbf{x}\|^2}$



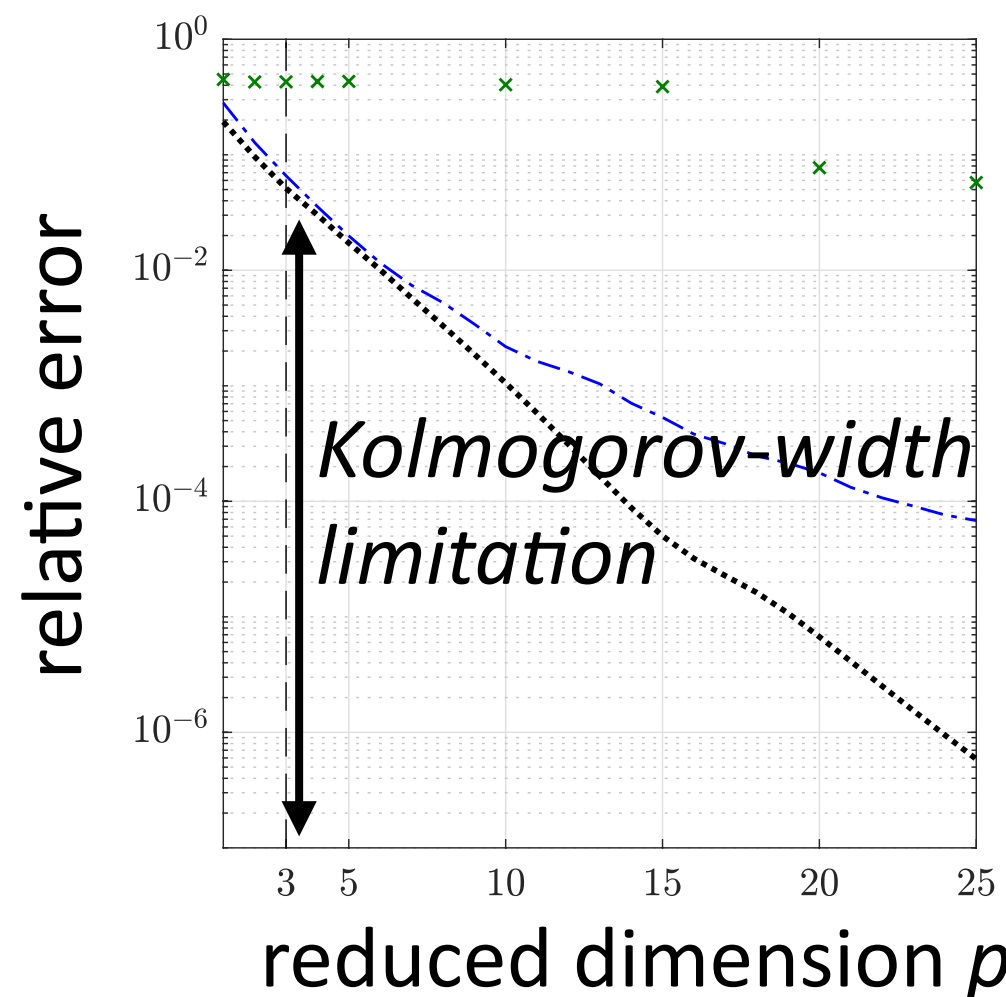
.....  $\tilde{d}_p(\mathcal{M})$

---  $P_2(\mathcal{M}, \text{range}(\boldsymbol{\Phi}))$

$\times \frac{\sqrt{\sum_{\mathbf{x} \in \mathcal{M}} \|\mathbf{x} - \tilde{\mathbf{x}}_{\text{LSPG}}\|^2}}{\sqrt{\sum_{\mathbf{x} \in \mathcal{M}} \|\mathbf{x}\|^2}}$

# Kolmogorov-width limitation of linear subspaces

- $\mathcal{M} := \{\mathbf{x}(t, \boldsymbol{\mu}) \mid t \in [0, T_{\text{final}}], \boldsymbol{\mu} \in \mathcal{D}\}$ : solution manifold
- $\mathcal{S}_p$ : set of all  $p$ -dimensional linear subspaces
- $\tilde{d}_p(\mathcal{M}) := \inf_{\mathcal{S} \in \mathcal{S}_p} P_2(\mathcal{M}, \mathcal{S})$ ,  $P_2(\mathcal{M}, \mathcal{S}) := \sqrt{\sum_{\mathbf{x} \in \mathcal{M}} \inf_{\mathbf{y} \in \mathcal{S}} \|\mathbf{x} - \mathbf{y}\|^2} / \sqrt{\sum_{\mathbf{x} \in \mathcal{M}} \|\mathbf{x}\|^2}$



$\cdots \tilde{d}_p(\mathcal{M})$   
 $- - - P_2(\mathcal{M}, \text{range}(\boldsymbol{\Phi}))$   
 $\times \frac{\sqrt{\sum_{\mathbf{x} \in \mathcal{M}} \|\mathbf{x} - \tilde{\mathbf{x}}_{\text{LSPG}}\|^2}}{\sqrt{\sum_{\mathbf{x} \in \mathcal{M}} \|\mathbf{x}\|^2}}$   
 $| \dim(\mathcal{M})$

- Kolmogorov-width limitation: **significant error** for  $p = \dim(\mathcal{M})$

**Goal:** overcome limitation via projection onto a nonlinear manifold



# Overcoming Kolmogorov-width limitation

## Transform/update the linear subspace

[Ohlberger and Rave, 2013; Iollo and Lombardi, 2014; Gerbeau and Lombardi, 2014; Peherstorfer and Willcox, 2015; Welper, 2017; Mojgani and Balajewicz, 2017; Reiss et al., 2018; Zimmermann et al., 2018; Peherstorfer, 2018; Rim and Mandli, 2018; Rim and Mandli, 2018; Nair and Balajewicz, 2019; Cagniard et al., 2019]

- + Can work much better than a fixed basis
- Some require **problem-specific knowledge or characteristics**
- Do not consider manifolds of **general nonlinear structure**

# Overcoming Kolmogorov-width limitation

## Transform/update the linear subspace

[Ohlberger and Rave, 2013; Iollo and Lombardi, 2014; Gerbeau and Lombardi, 2014; Peherstorfer and Willcox, 2015; Welper, 2017; Mojgani and Balajewicz, 2017; Reiss et al., 2018; Zimmermann et al., 2018; Peherstorfer, 2018; Rim and Mandli, 2018; Rim and Mandli, 2018; Nair and Balajewicz, 2019; Cagniard et al., 2019]

- + Can work much better than a fixed basis
- Some require **problem-specific knowledge or characteristics**
- Do not consider manifolds of **general nonlinear structure**

## ***A priori* construction of local linear subspaces**

[Dihlmann et al., 2011; Drohmann et al., 2011; Amsallem, Zahr, Farhat, 2012; Peherstorfer et al., 2014; Taddei et al., 2015]

- + **Tailored bases** for local regions of space/time domain, state space
- Do not consider manifolds of **general nonlinear structure**

# Overcoming Kolmogorov-width limitation

## Transform/update the linear subspace

[Ohlberger and Rave, 2013; Iollo and Lombardi, 2014; Gerbeau and Lombardi, 2014; Peherstorfer and Willcox, 2015; Welper, 2017; Mojgani and Balajewicz, 2017; Reiss et al., 2018; Zimmermann et al., 2018; Peherstorfer, 2018; Rim and Mandli, 2018; Rim and Mandli, 2018; Nair and Balajewicz, 2019; Cagniard et al., 2019]

- + Can work much better than a fixed basis
- Some require **problem-specific knowledge or characteristics**
- Do not consider manifolds of **general nonlinear structure**

## *A priori* construction of local linear subspaces

[Dihlmann et al., 2011; Drohmann et al., 2011; Amsallem, Zahr, Farhat, 2012; Peherstorfer et al., 2014; Taddei et al., 2015]

- + **Tailored bases** for local regions of space/time domain, state space
- Do not consider manifolds of **general nonlinear structure**

## Model reduction on nonlinear manifolds [Gu, 2011; Kashima, 2016; Hartman and Mestha, 2017]

- **Kinematically inconsistent** [Kashima, 2016; Hartman and Mestha, 2017]
- **Limited** to piecewise linear manifolds [Gu, 2011]
- Solutions **lack optimality** [Gu, 2011; Kashima, 2016; Hartman and Mestha, 2017]

## Overcome shortcomings of existing methods

- + Enable manifolds with **general nonlinear structure**
- + **Kinematically consistent**
- + Satisfy **optimality property**

*Manifold Galerkin and LSPG projection*

## Practical nonlinear-manifold construction

- + **No problem-specific knowledge** required
- + Use **same training data** as POD

*Deep convolutional autoencoders*

## Overcome shortcomings of existing methods

- + Enable manifolds with **general nonlinear structure**
- + **Kinematically consistent**
- + Satisfy **optimality property**

### *Manifold Galerkin and LSPG projection*

## Practical nonlinear-manifold construction

- + No problem-specific knowledge required
- + Use same training data as POD

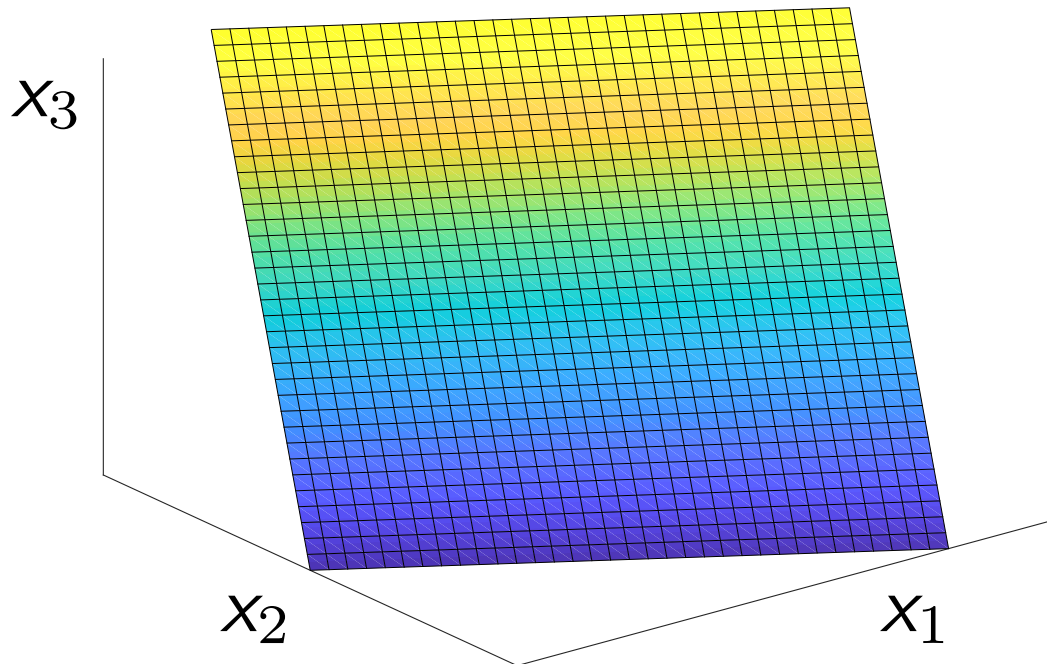
### *Deep convolutional autoencoders*

# Nonlinear trial manifold

## Linear trial subspace

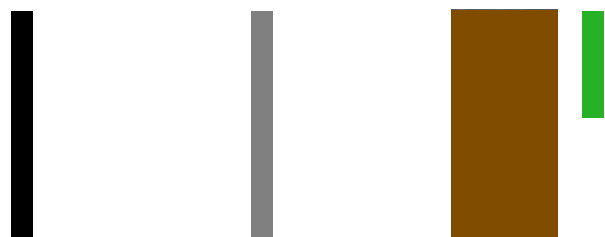
$$\text{range}(\Phi) := \{\Phi \hat{\mathbf{x}} \mid \hat{\mathbf{x}} \in \mathbb{R}^p\}$$

example  
 $N=3$   
 $p=2$



state

$$\mathbf{x}(t) \approx \tilde{\mathbf{x}}(t) = \Phi \hat{\mathbf{x}}(t) \in \text{range}(\Phi)$$

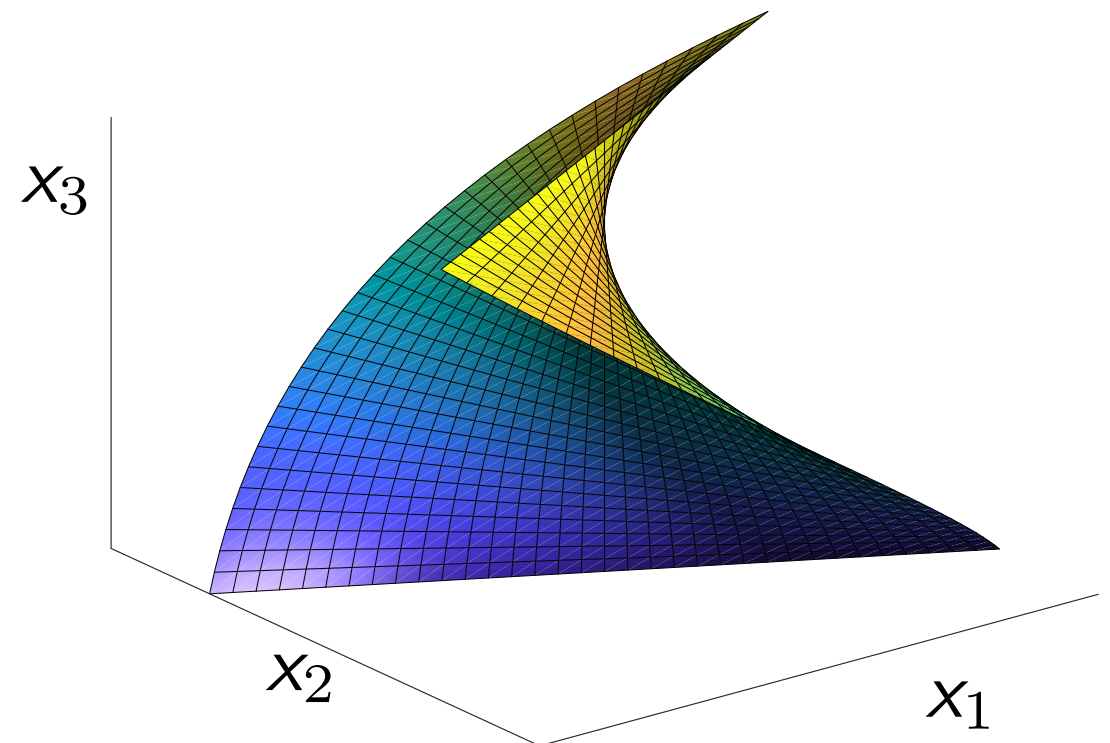


velocity

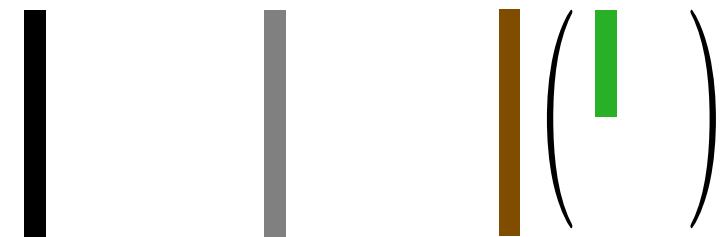
$$\frac{d\mathbf{x}}{dt} \approx \frac{d\tilde{\mathbf{x}}}{dt} = \Phi \frac{d\hat{\mathbf{x}}}{dt} \in \text{range}(\Phi)$$

## Nonlinear trial manifold

$$\mathcal{S} := \{\mathbf{g}(\hat{\mathbf{x}}) \mid \hat{\mathbf{x}} \in \mathbb{R}^p\}$$



$$\mathbf{x}(t) \approx \tilde{\mathbf{x}}(t) = \mathbf{g}(\hat{\mathbf{x}}(t)) \in \mathcal{S}$$



+ Manifold has general structure

$$\frac{d\mathbf{x}}{dt} \approx \frac{d\tilde{\mathbf{x}}}{dt} = \nabla \mathbf{g}(\hat{\mathbf{x}}) \frac{d\hat{\mathbf{x}}}{dt} \in T_{\hat{\mathbf{x}}} \mathcal{S}$$

+ Kinematically consistent



1. *Training*: Solve ODE for  $\mu \in \mathcal{D}_{\text{training}}$  and collect simulation data
2. *Machine learning*: Identify structure in data
3. *Reduction*: Reduce the cost of solving ODE for  $\mu \in \mathcal{D}_{\text{query}} \setminus \mathcal{D}_{\text{training}}$

## Linear-subspace ROM

Given  $\Phi$

*Galerkin*  $\frac{d\hat{\mathbf{x}}}{dt} = \underset{\hat{\mathbf{v}} \in \mathbb{R}^p}{\operatorname{argmin}} \|\mathbf{r}(\Phi \hat{\mathbf{v}}, \Phi \hat{\mathbf{x}}; t)\|_2$

$$\Updownarrow$$
$$\frac{d\hat{\mathbf{x}}}{dt} = \Phi^T \mathbf{f}(\Phi \hat{\mathbf{x}}; t)$$

*LSPG*

$$\hat{\mathbf{x}}^n = \underset{\hat{\mathbf{v}} \in \mathbb{R}^p}{\operatorname{argmin}} \|\mathbf{r}^n(\Phi \hat{\mathbf{v}})\|_2$$

## Nonlinear-manifold ROM

Given  $\mathbf{g}(\hat{\mathbf{x}})$

$$\frac{d\hat{\mathbf{x}}}{dt} = \underset{\hat{\mathbf{v}} \in \mathbb{R}^p}{\operatorname{argmin}} \|\mathbf{r}(\nabla \mathbf{g}(\hat{\mathbf{x}}) \hat{\mathbf{v}}, \mathbf{g}(\hat{\mathbf{x}}); t)\|_2$$
$$\Updownarrow$$
$$\frac{d\hat{\mathbf{x}}}{dt} = \nabla \mathbf{g}(\hat{\mathbf{x}})^+ \mathbf{f}(\mathbf{g}(\hat{\mathbf{x}}); t)$$

$$\hat{\mathbf{x}}^n = \underset{\hat{\mathbf{v}} \in \mathbb{R}^p}{\operatorname{argmin}} \|\mathbf{r}^n(\mathbf{g}(\hat{\mathbf{v}}))\|_2$$

+ Satisfy residual minimization

### Theorem [Lee, C., 2020]

Manifold Galerkin and manifold LSPG are equivalent if

1. the nonlinear trial manifold  $\mathcal{S}$  is twice continuously differentiable,
2.  $\|\hat{\mathbf{x}}^{n-j} - \hat{\mathbf{x}}^n\| = O(\Delta t)$  for  $n = 1, \dots, T$  and  $j = 1, \dots, k$ , and
3. the limit  $\Delta t \rightarrow 0$  is taken.



# Error bound

## Theorem [Lee, C., 2020]

If the following conditions hold:

1.  $\mathbf{f}(\cdot; t)$  is Lipschitz continuous with Lipschitz constant  $\kappa$
2.  $\Delta t$  is small enough such that  $0 < h := |\alpha_0| - |\beta_0|\kappa\Delta t$ , then

$$\|\mathbf{x}^n - \mathbf{g}(\hat{\mathbf{x}}_G^n)\|_2 \leq \frac{1}{h} \|\mathbf{r}_G^n(\mathbf{g}(\hat{\mathbf{x}}_G))\|_2 + \frac{1}{h} \sum_{\ell=1}^k |\gamma_\ell| \|\mathbf{x}^{n-\ell} - \mathbf{g}(\hat{\mathbf{x}}_G)\|_2$$
$$\|\mathbf{x}^n - \mathbf{g}(\hat{\mathbf{x}}_{\text{LSPG}}^n)\|_2 \leq \frac{1}{h} \min_{\hat{\mathbf{v}}} \|\mathbf{r}_{\text{LSPG}}^n(\mathbf{g}(\hat{\mathbf{v}}))\|_2 + \frac{1}{h} \sum_{\ell=1}^k |\gamma_\ell| \|\mathbf{x}^{n-\ell} - \mathbf{g}(\hat{\mathbf{x}}_{\text{LSPG}})\|_2$$

+ Manifold LSPG sequentially minimizes the error bound

***How to construct manifold  $\mathcal{S} := \{\mathbf{g}(\hat{\mathbf{x}}) \mid \hat{\mathbf{x}} \in \mathbb{R}^p\}$  from training data?***

## Overcome shortcomings of existing methods

- + Enable manifolds with general nonlinear structure
- + Kinematically consistent
- + Satisfy optimality property

*Manifold Galerkin and LSPG projection*

## Practical nonlinear-manifold construction

- + No problem-specific knowledge required
- + Use same training data as POD

*Deep convolutional autoencoders*

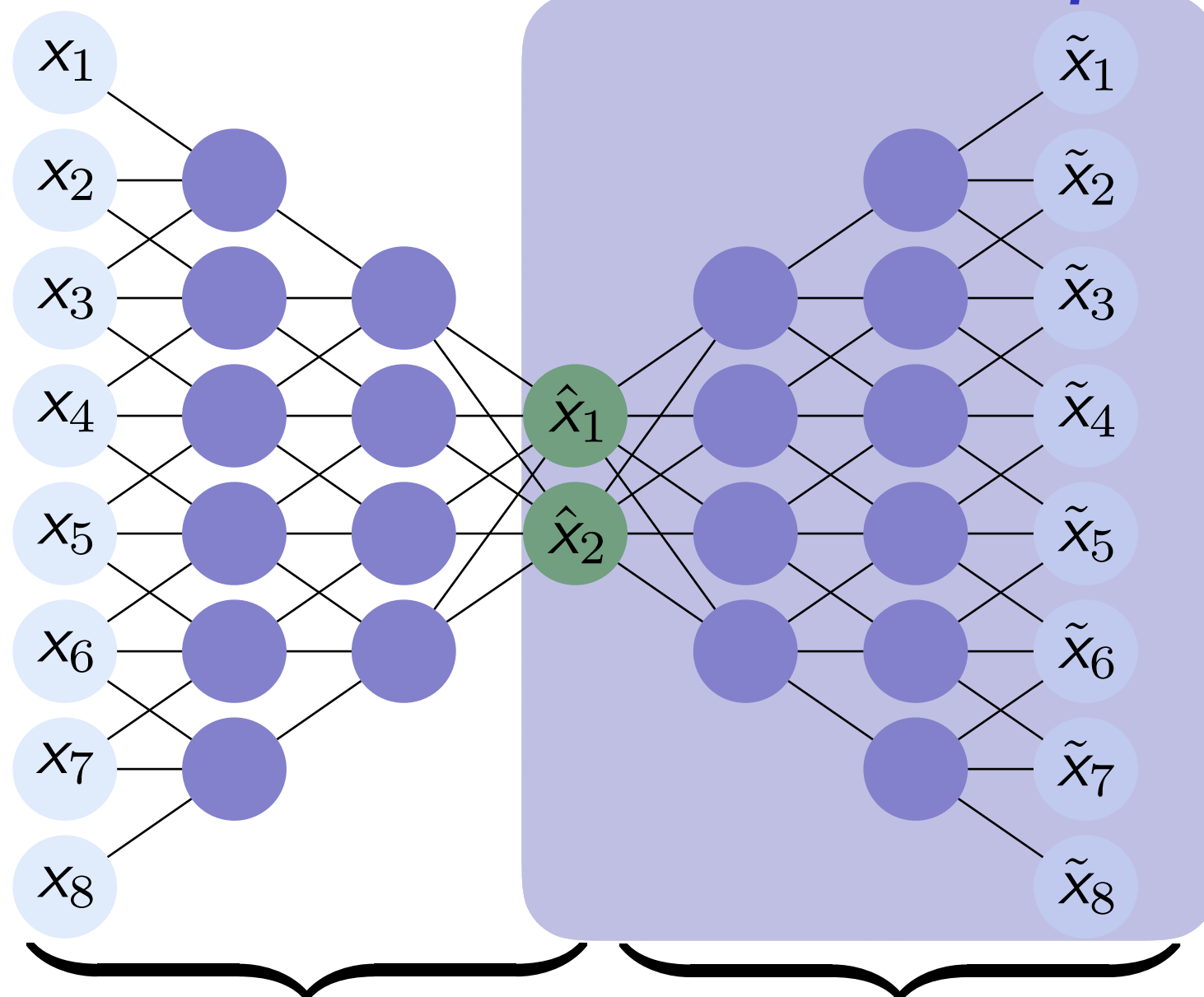
$$\mathcal{S} := \{\mathbf{g}(\hat{\mathbf{x}}) \mid \hat{\mathbf{x}} \in \mathbb{R}^p\}$$

# Deep autoencoders

*Input layer*

*Code*

*Output layer*



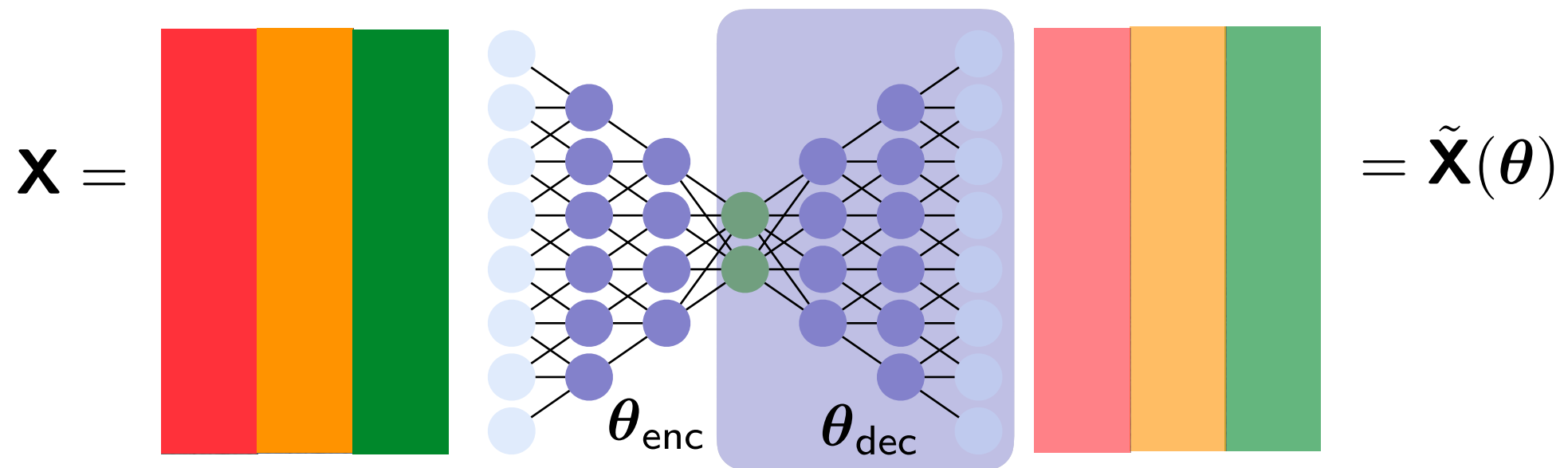
**Encoder**  $\mathbf{h}_{\text{enc}}(\cdot; \boldsymbol{\theta}_{\text{enc}})$  **Decoder**  $\mathbf{h}_{\text{dec}}(\cdot; \boldsymbol{\theta}_{\text{dec}})$

$$\tilde{\mathbf{x}} = \mathbf{h}_{\text{dec}}(\cdot; \boldsymbol{\theta}_{\text{dec}}) \circ \mathbf{h}_{\text{enc}}(\mathbf{x}; \boldsymbol{\theta}_{\text{enc}})$$

+ If  $\tilde{\mathbf{x}} \approx \mathbf{x}$  for  $\boldsymbol{\theta}_{\text{dec}}^*$ , then  $\mathbf{g} = \mathbf{h}_{\text{dec}}(\cdot; \boldsymbol{\theta}_{\text{dec}}^*)$  is accurate manifold parameterization



1. *Training*: Solve ODE for  $\mu \in \mathcal{D}_{\text{training}}$  and collect simulation data
2. *Machine learning*: Identify structure in data
3. *Reduction*: Reduce the cost of solving ODE for  $\mu \in \mathcal{D}_{\text{query}} \setminus \mathcal{D}_{\text{training}}$



- Compute  $\theta^*$  by approximately solving  $\underset{\theta}{\text{minimize}} \|\mathbf{X} - \tilde{\mathbf{X}}(\theta)\|_F$
- Define nonlinear trial manifold by setting  $\mathbf{g} = \mathbf{h}_{\text{dec}}(\cdot; \theta_{\text{dec}}^*)$
- + Same snapshot data, no specialized problem knowledge



1. *Training*: Solve ODE for  $\mu \in \mathcal{D}_{\text{training}}$  and collect simulation data
2. *Machine learning*: Identify structure in data
3. *Reduction*: Reduce the cost of solving ODE for  $\mu \in \mathcal{D}_{\text{query}} \setminus \mathcal{D}_{\text{training}}$

## Subspace ROM

Given  $\Phi$

*Galerkin*  $\frac{d\hat{\mathbf{x}}}{dt} = \operatorname{argmin}_{\hat{\mathbf{v}} \in \mathbb{R}^p} \|\mathbf{r}(\Phi \hat{\mathbf{v}}, \Phi \hat{\mathbf{x}}; t)\|_2$



$$\frac{d\hat{\mathbf{x}}}{dt} = \Phi^T \mathbf{f}(\Phi \hat{\mathbf{x}}; t)$$

*LSPG*

$$\hat{\mathbf{x}}^n = \operatorname{argmin}_{\hat{\mathbf{v}} \in \mathbb{R}^p} \|\mathbf{r}^n(\Phi \hat{\mathbf{v}})\|_2$$

## Manifold ROM

Given  $\mathbf{g}(\hat{\mathbf{x}})$

$$\frac{d\hat{\mathbf{x}}}{dt} = \operatorname{argmin}_{\hat{\mathbf{v}} \in \mathbb{R}^p} \|\mathbf{r}(\nabla \mathbf{g}(\hat{\mathbf{x}}) \hat{\mathbf{v}}, \mathbf{g}(\hat{\mathbf{x}}); t)\|_2$$



$$\frac{d\hat{\mathbf{x}}}{dt} = \nabla \mathbf{g}(\hat{\mathbf{x}})^+ \mathbf{f}(\mathbf{g}(\hat{\mathbf{x}}); t)$$

$$\hat{\mathbf{x}}^n = \operatorname{argmin}_{\hat{\mathbf{v}} \in \mathbb{R}^p} \|\mathbf{r}^n(\mathbf{g}(\hat{\mathbf{v}}))\|_2$$

- + Satisfy residual minimization
- + Predictions directly integrate deep learning with computational physics

# Numerical results

## 1D Burgers' equation

$$\frac{\partial w(x, t; \mu)}{\partial t} + \frac{\partial f(w(x, t; \mu))}{\partial x} = 0.02e^{\alpha x}$$

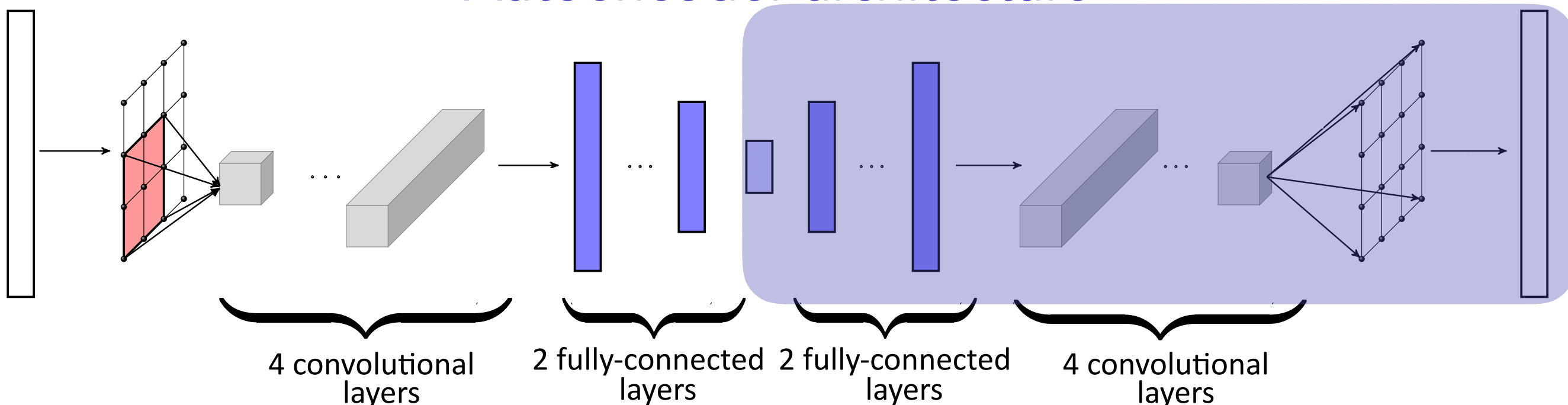
- $\mu$ :  $\alpha$ , inlet boundary condition
- *Spatial discretization*: finite volume
- *Time integrator*: backward Euler

## 2D reacting flow

$$\begin{aligned} \frac{\partial \mathbf{w}(\vec{x}, t; \mu)}{\partial t} = & \nabla \cdot (\kappa \nabla \mathbf{w}(\vec{x}, t; \mu)) \\ & - \mathbf{v} \cdot \nabla \mathbf{w}(\vec{x}, t; \mu) + \mathbf{q}(\mathbf{w}(\vec{x}, t; \mu); \mu) \end{aligned}$$

- $\mu$ : two terms in reaction
- *Spatial discretization*: finite difference
- *Time integrator*: BDF2

## Autoencoder architecture



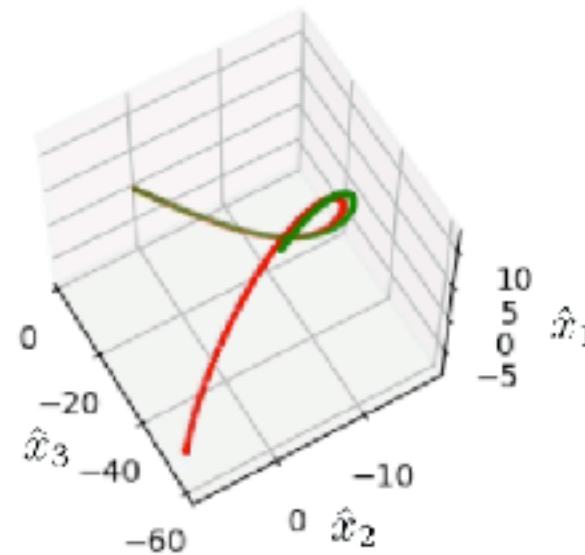
# Manifold interpretation: Burgers' equation

**FOM**

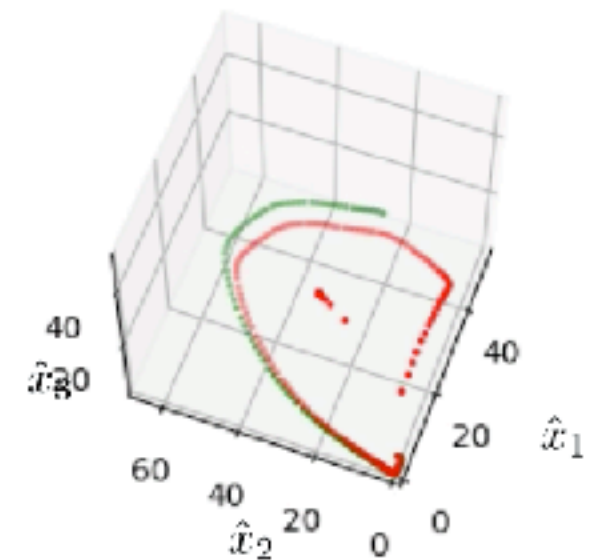
**POD,  $p=3$   
projection**

**Autoencoder,  $p=3$   
projection**

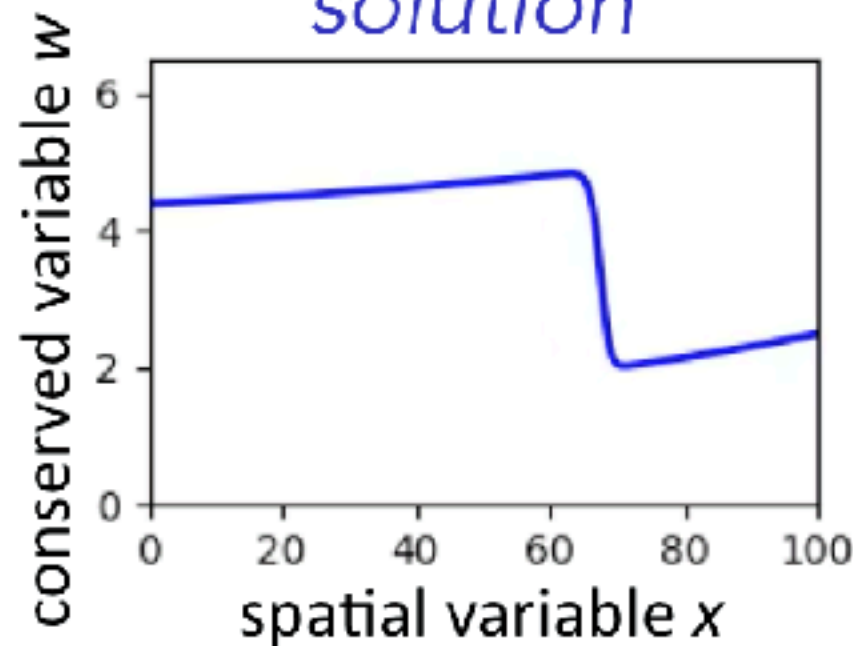
$t = 22.61, (\mu_1, \mu_2) = (4.39, 0.015)$



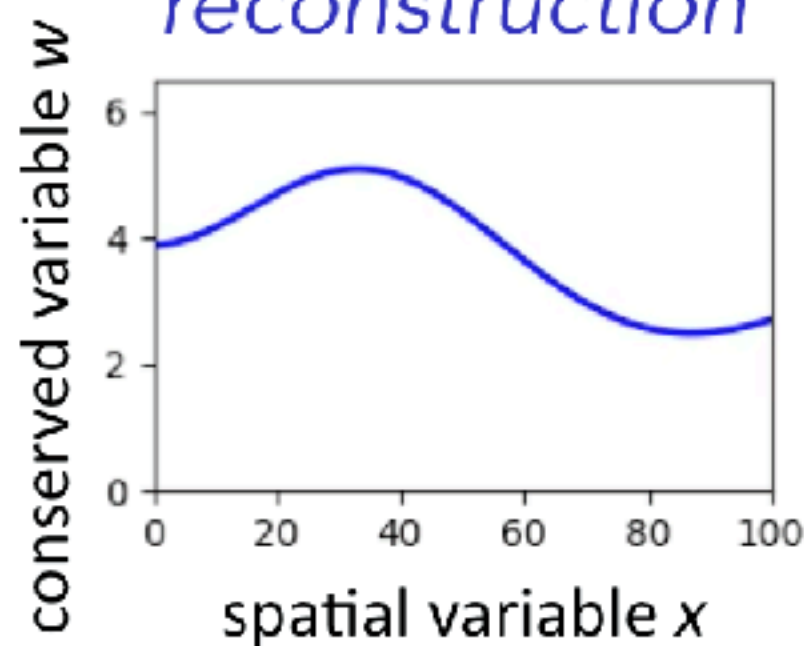
$t = 22.61, (\mu_1, \mu_2) = (4.39, 0.015)$



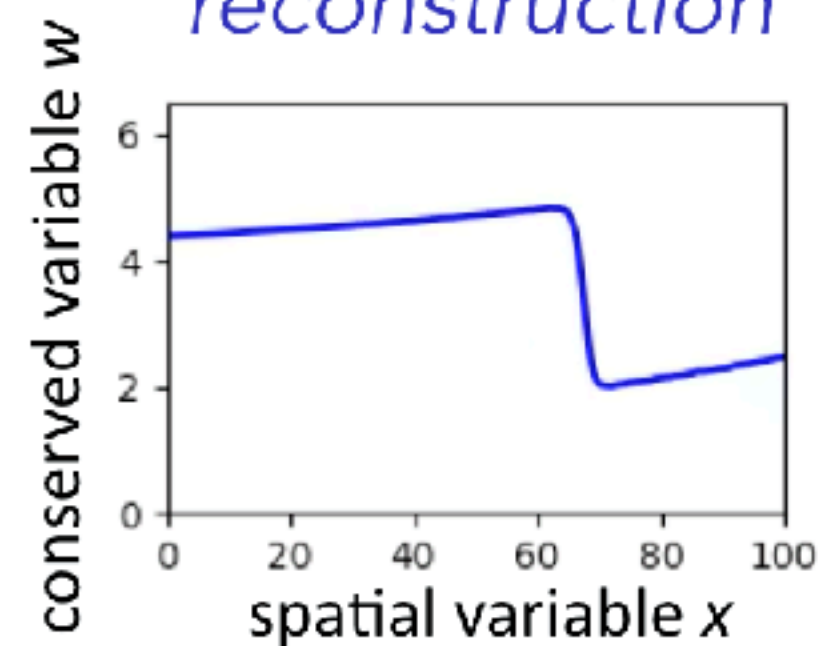
**solution**



**reconstruction**



**reconstruction**



+ Projection error onto 3-dimensional manifold **nearly perfect**



# Manifold LSPG outperforms optimal linear subspace

*1D Burgers' equation*

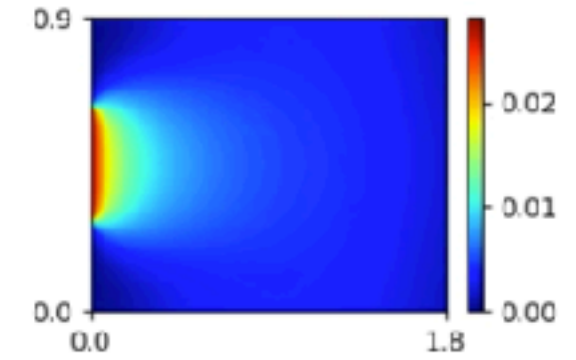
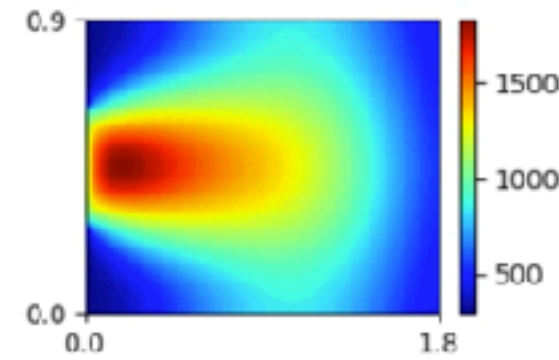
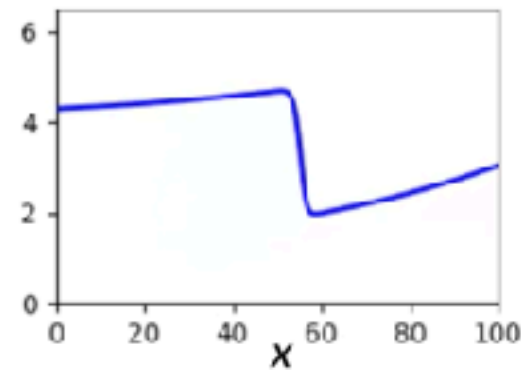
*2D reacting flow*

conserved variable

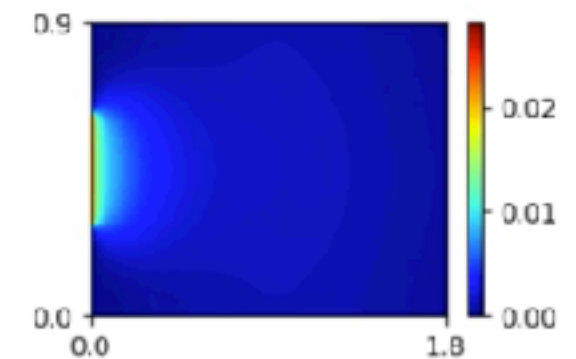
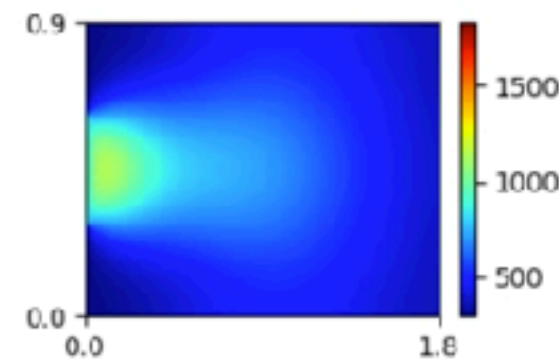
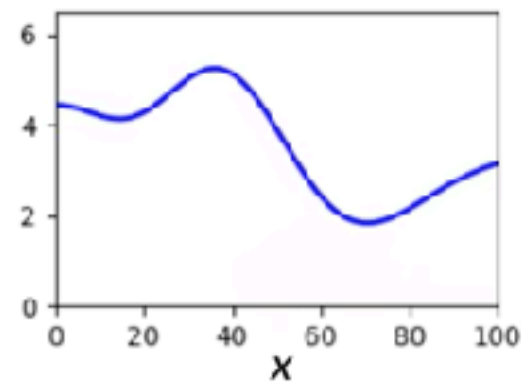
temperature

$H_2$  fraction

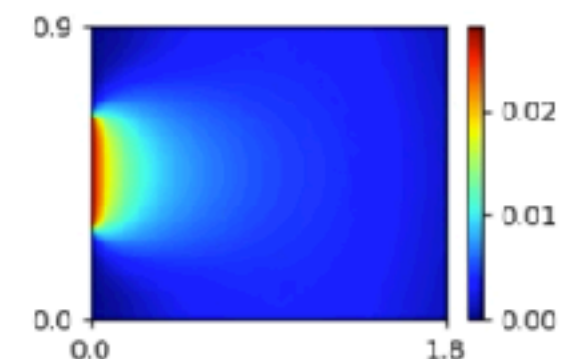
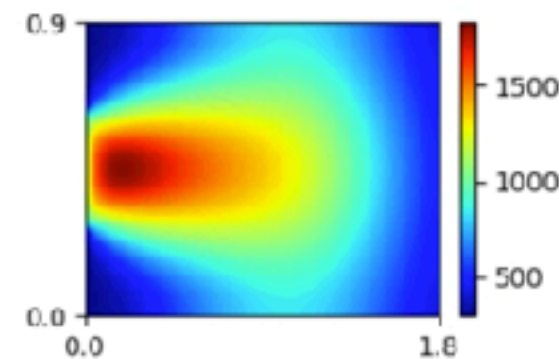
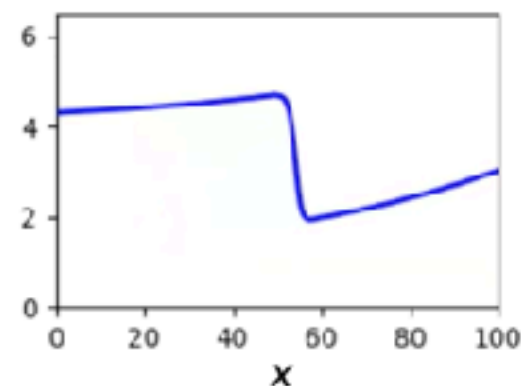
*high-fidelity  
model*



*POD-LSPG  
 $p=5$*

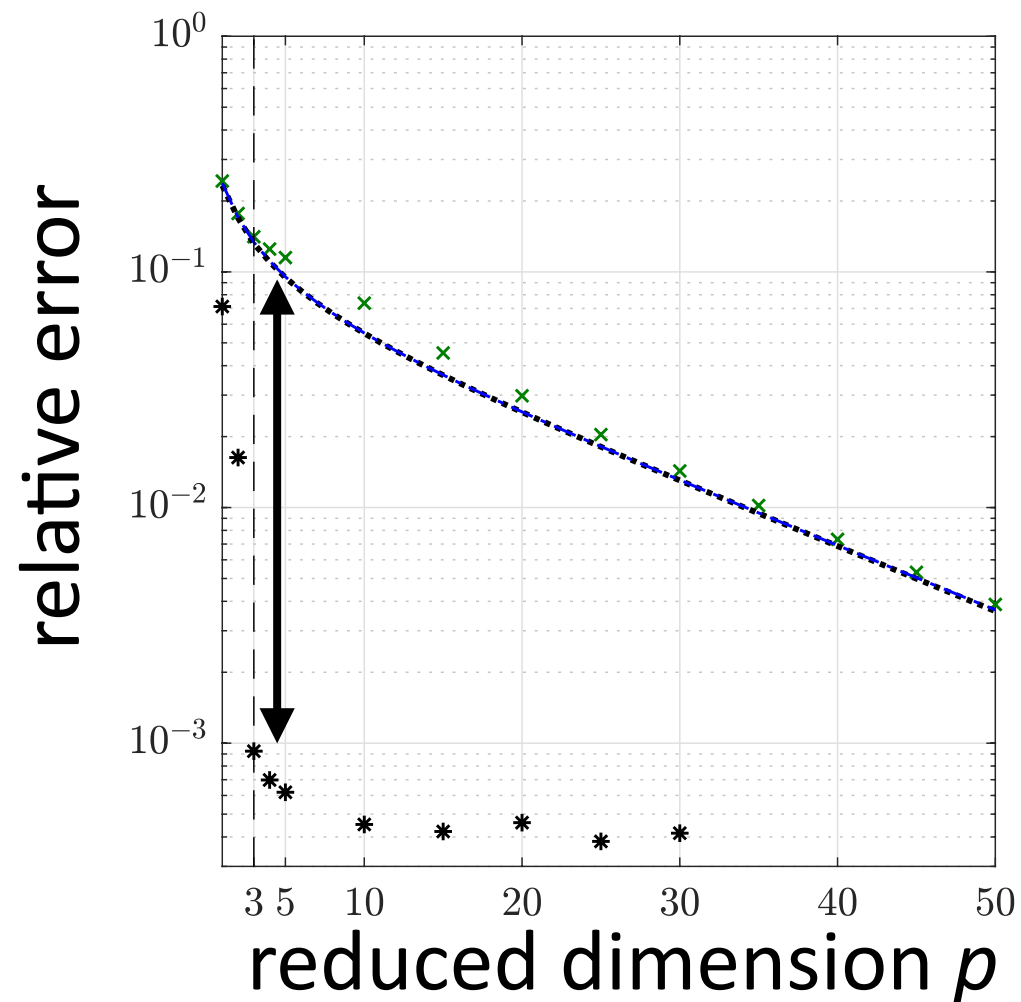


*Manifold LSPG  
 $p=5$*

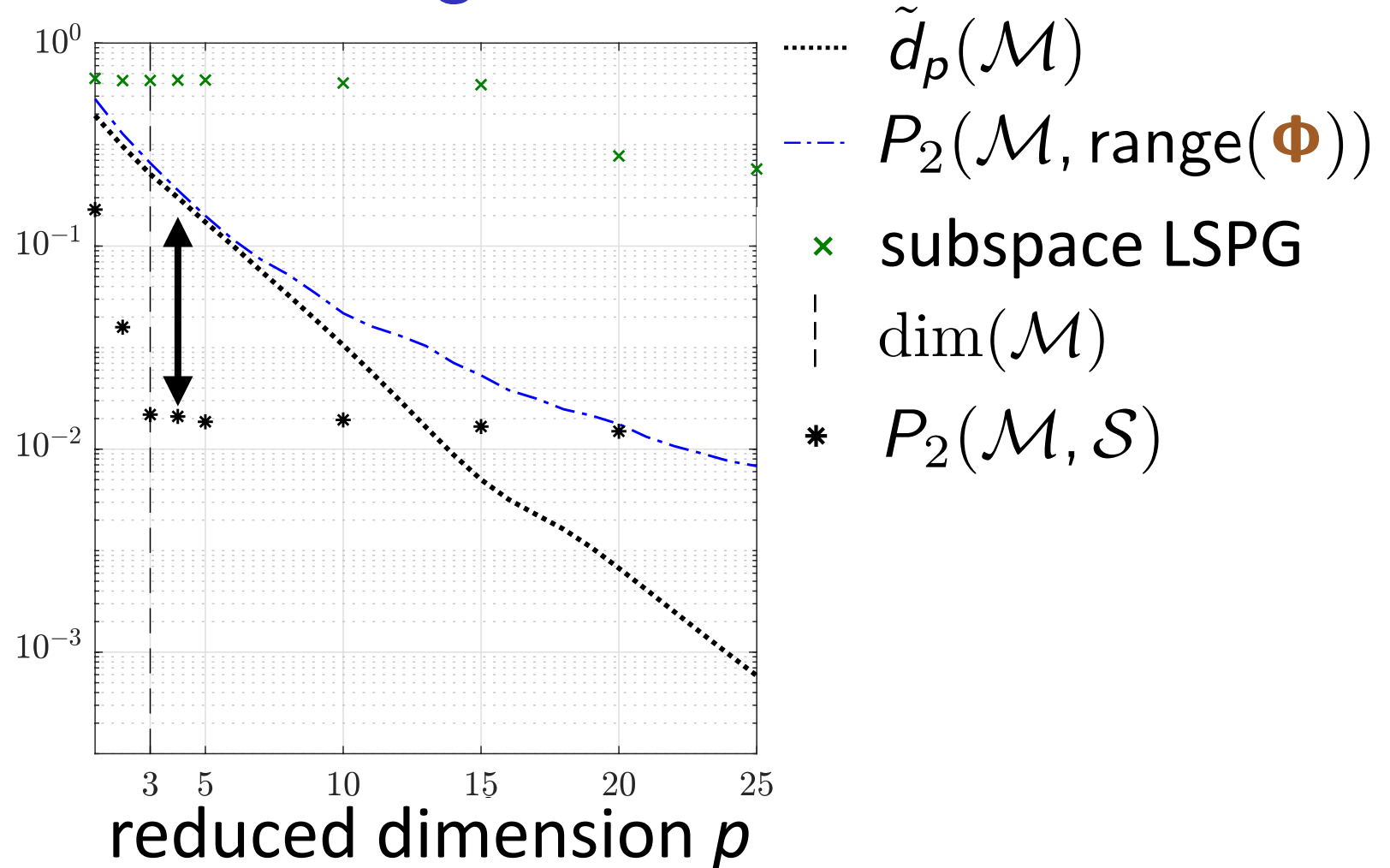


# Method improves generalization performance

*Burgers' equation*



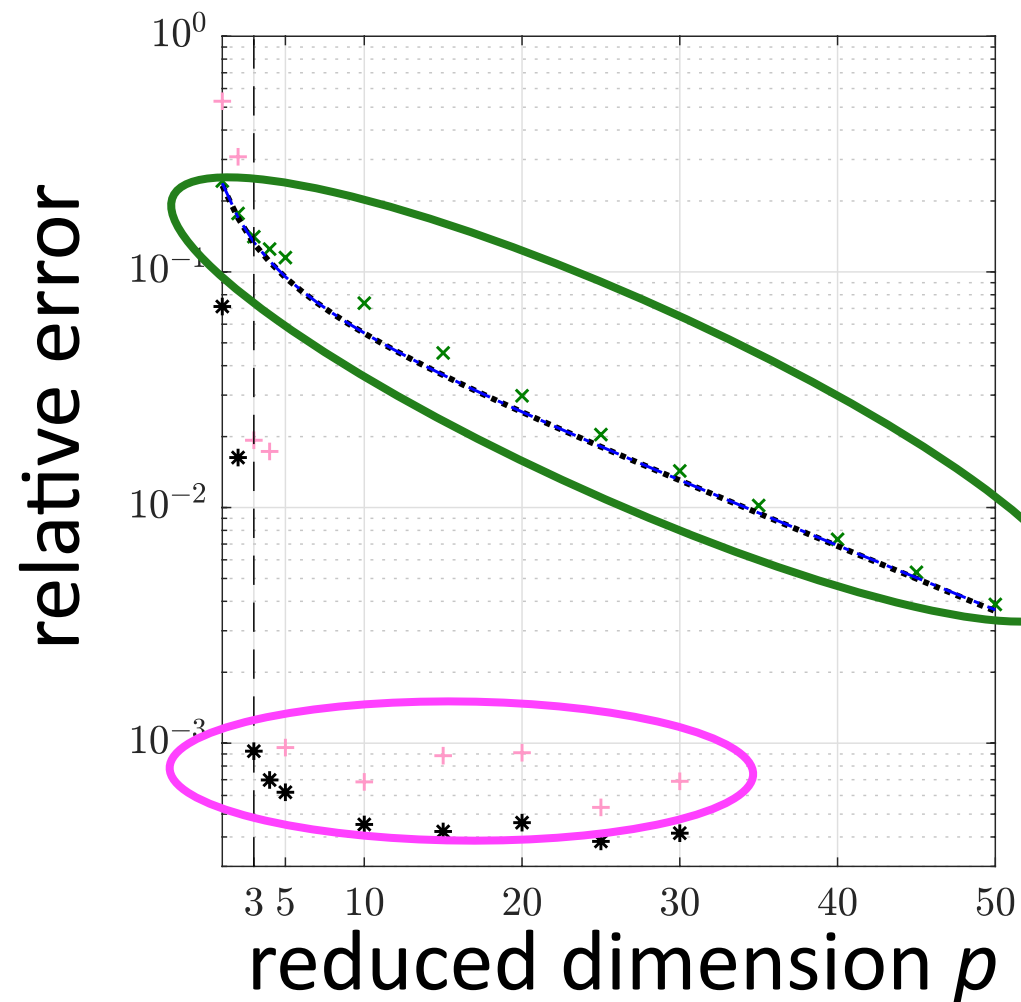
*Reacting flow*



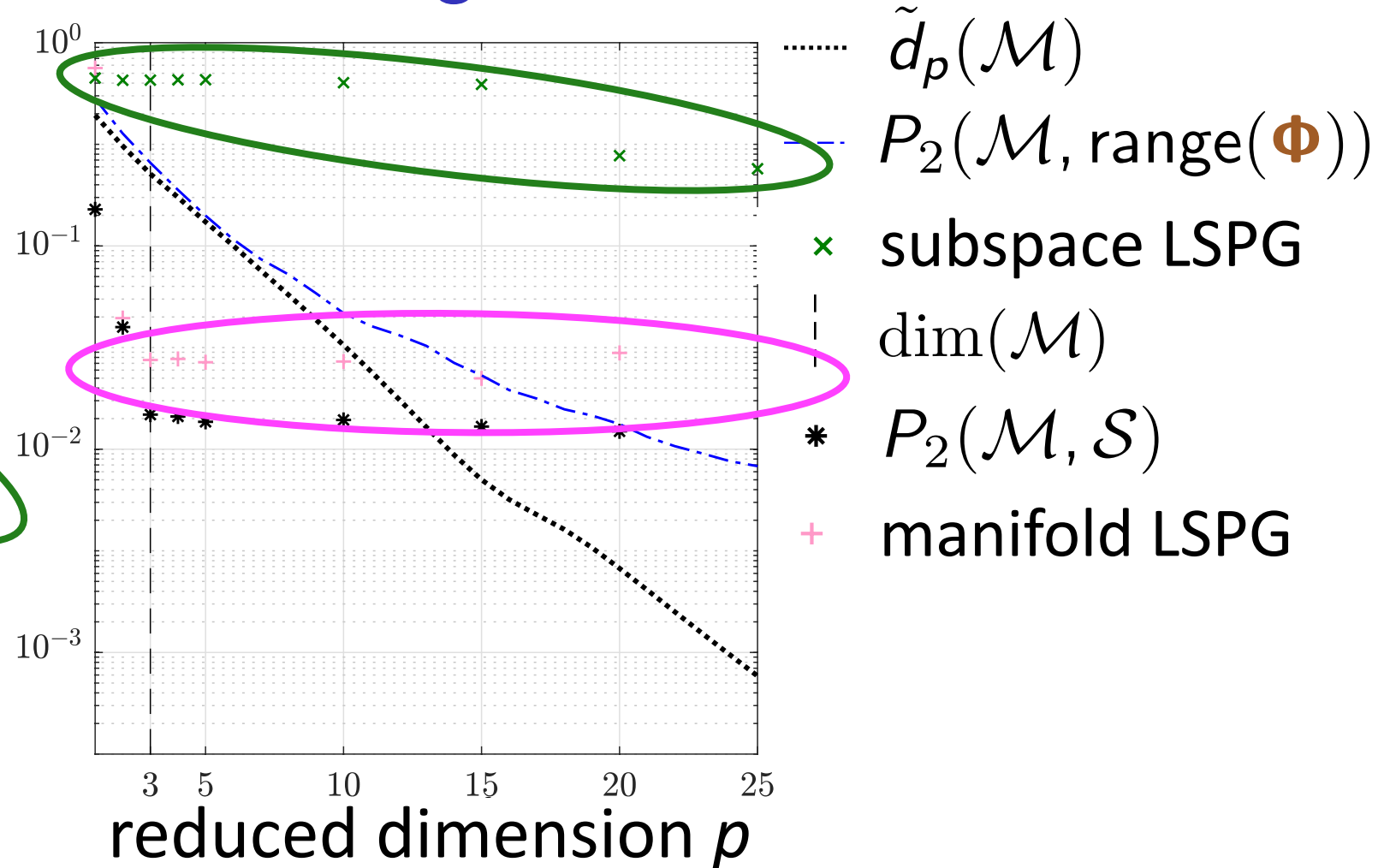
+ Autoencoder manifold **significantly better** than optimal linear subspace

# Method improves generalization performance

*Burgers' equation*



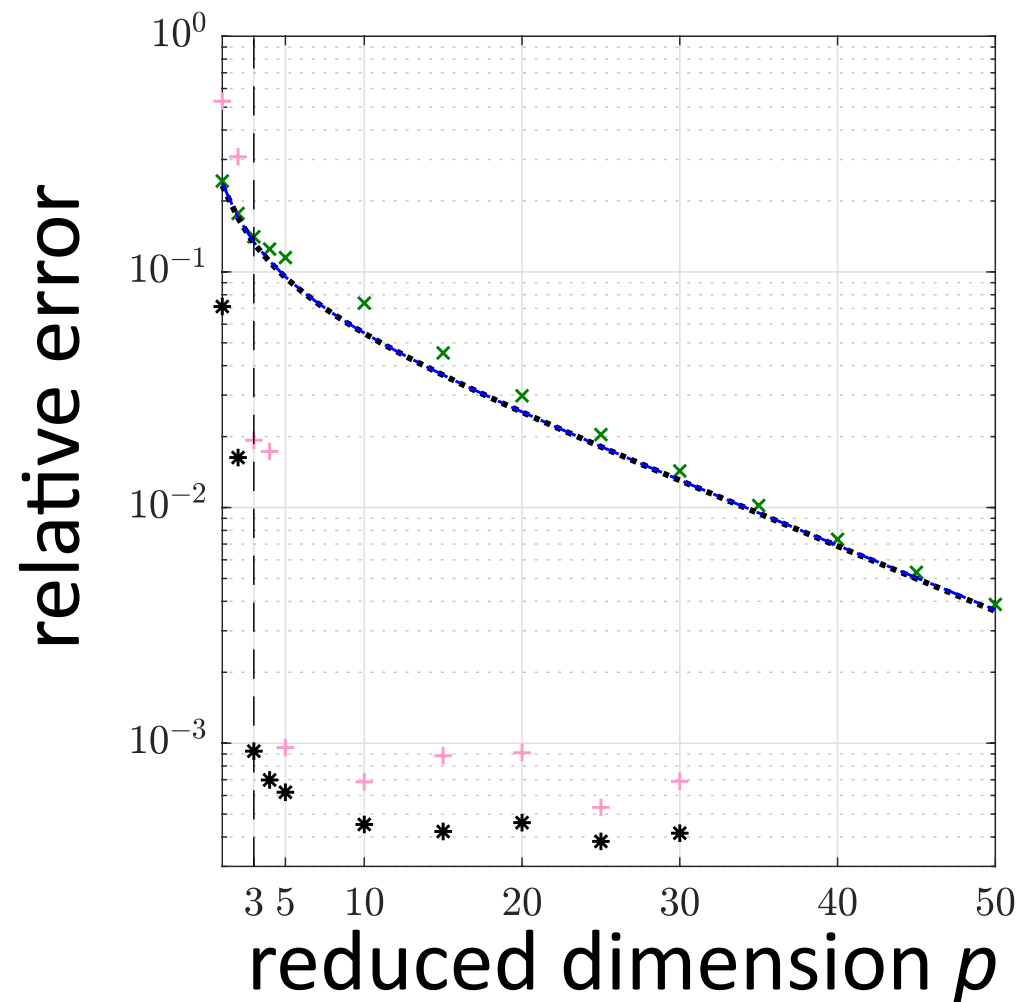
*Reacting flow*



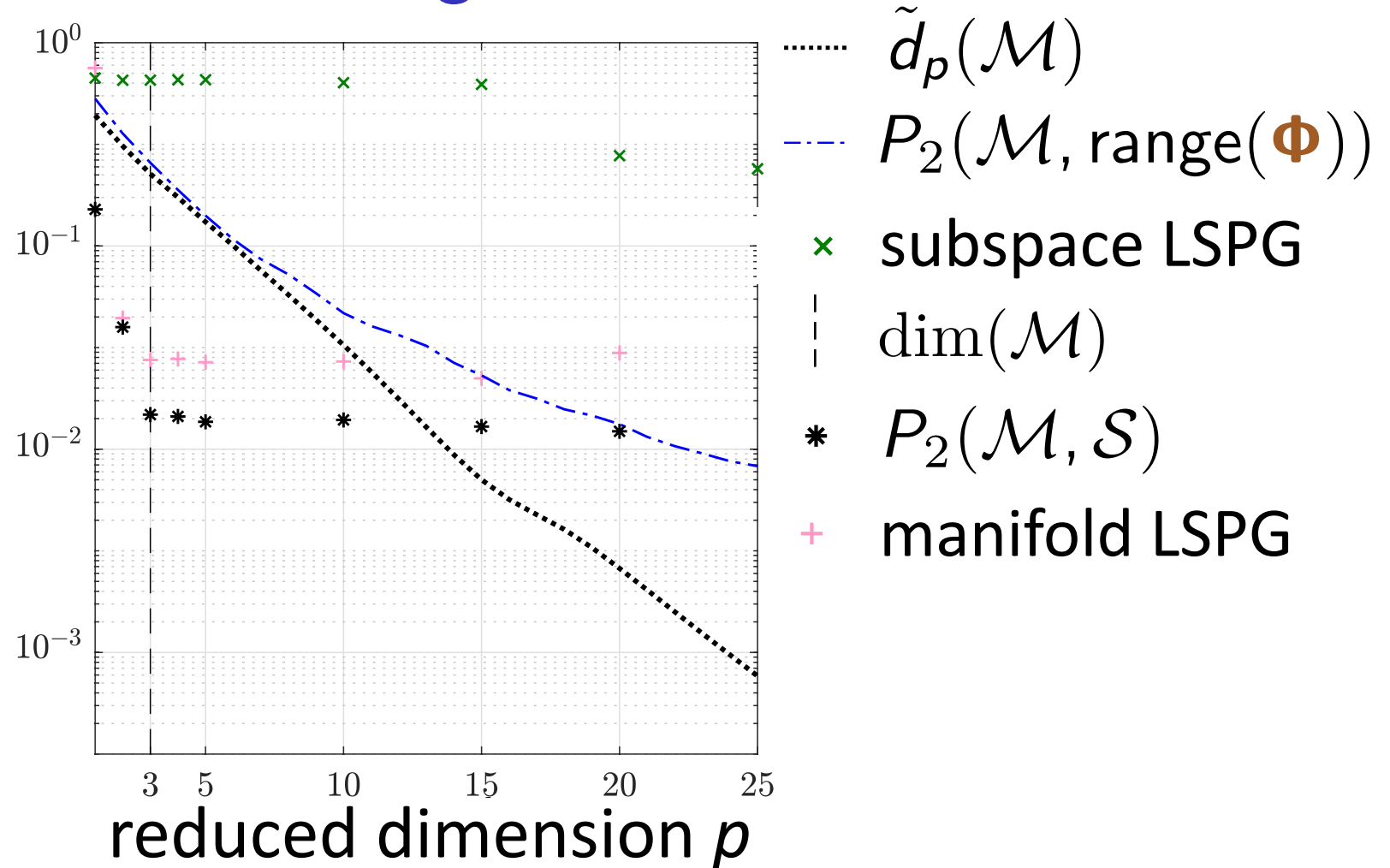
- + Autoencoder manifold significantly better than optimal linear subspace
- + Manifold LSPG orders-of-magnitude more accurate than subspace LSPG

# Method improves generalization performance

*Burgers' equation*



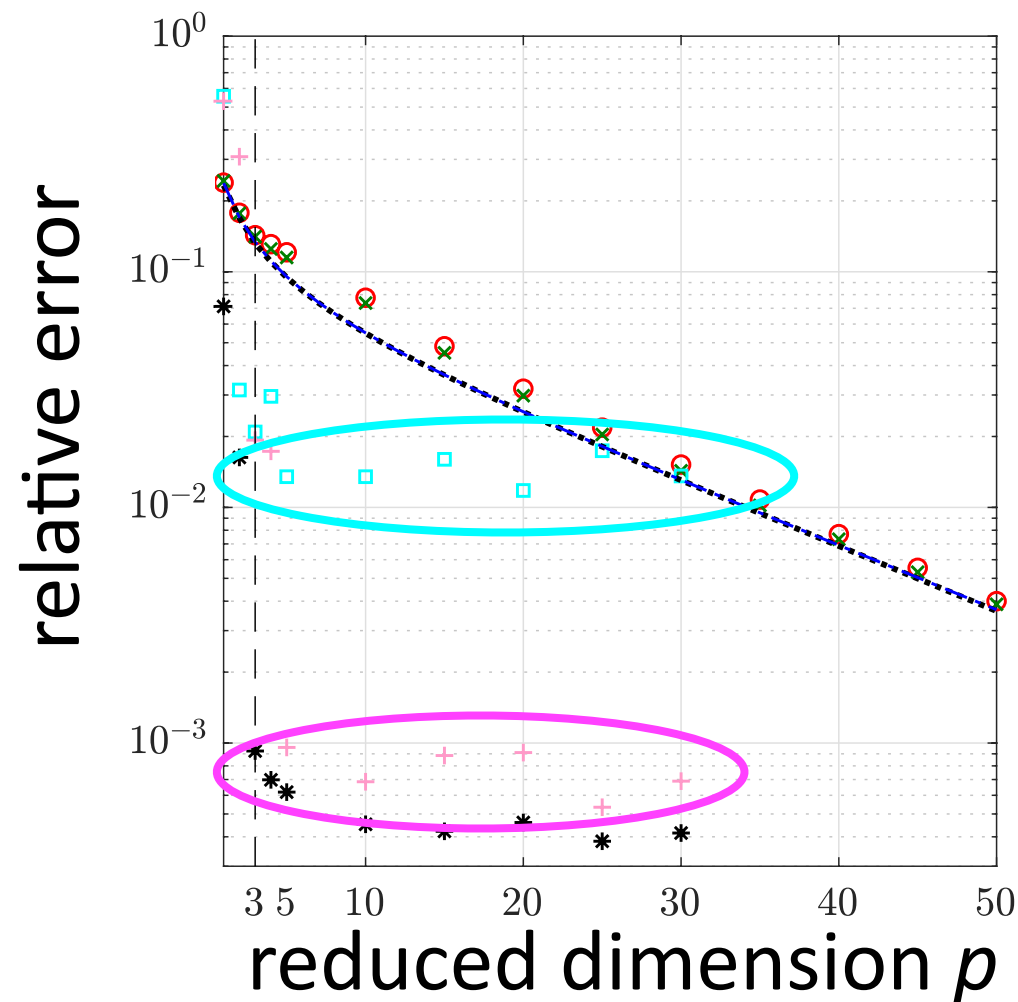
*Reacting flow*



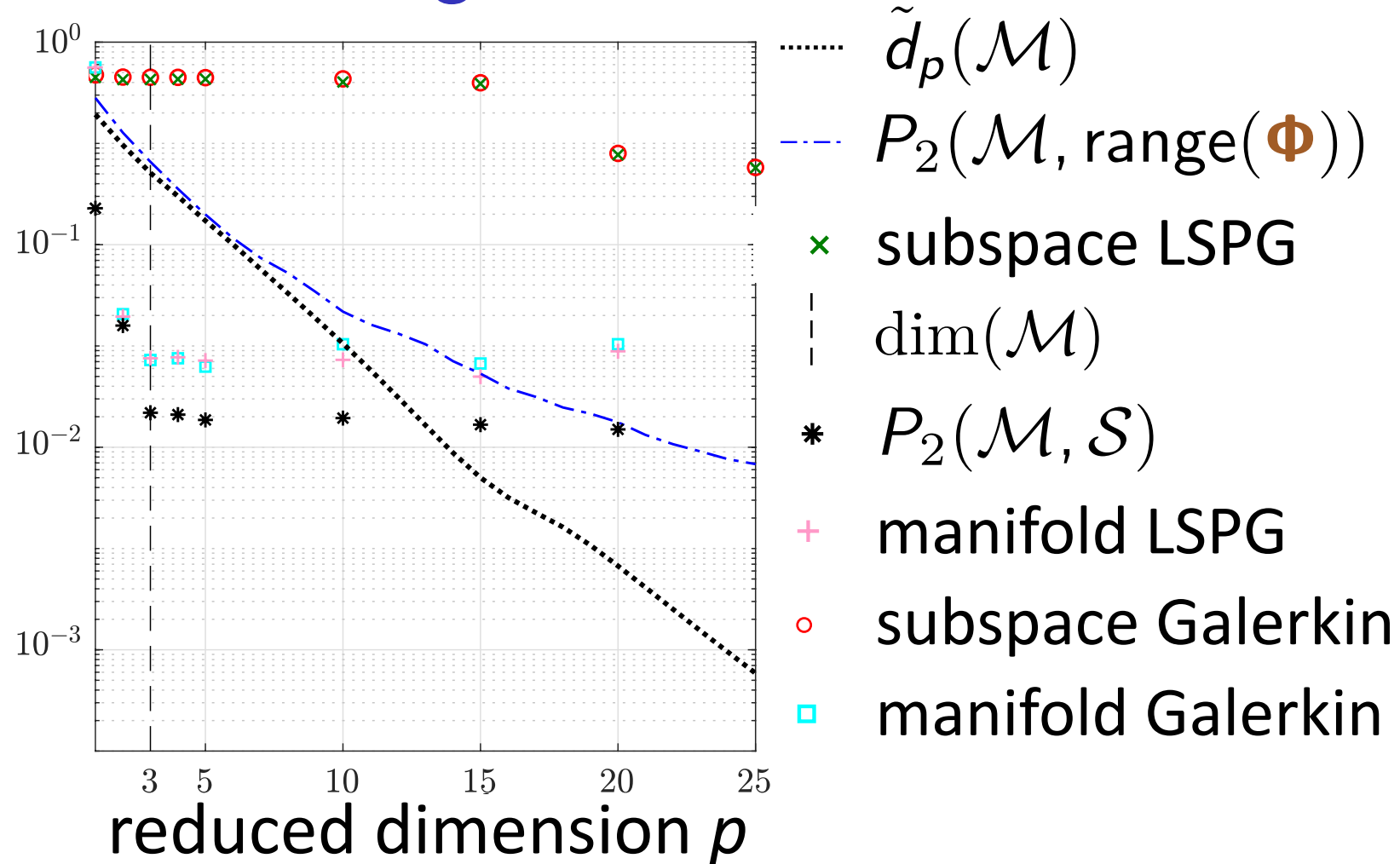
- + Autoencoder manifold significantly better than optimal linear subspace
- + Manifold LSPG orders-of-magnitude more accurate than subspace LSPG
- + Method breaks Kolmogorov-width barrier

# Method improves generalization performance

*Burgers' equation*



*Reacting flow*



- + Autoencoder manifold significantly better than optimal linear subspace
- + Manifold LSPG orders-of-magnitude more accurate than subspace LSPG
- + Method breaks Kolmogorov-width barrier
- + Manifold LSPG outperforms manifold Galerkin on 1D Burgers' equation

# Outstanding challenges in model reduction

## 1) Linear-subspace assumption is strong

$$\mathbf{x}(t) \approx \tilde{\mathbf{x}}(t) = \Phi \hat{\mathbf{x}}(t)$$

- Lee and C. “Model reduction of dynamical systems on nonlinear manifolds using deep convolutional autoencoders.” J Comp Phys, 404:108973, 2020.

## 2) Important physical properties not satisfied

<i>Galerkin</i>	<i>LSPG</i>
$\Phi \frac{d\hat{\mathbf{x}}}{dt}(\mathbf{x}, t) = \operatorname{argmin}_{\mathbf{v} \in \operatorname{range}(\Phi)} \ \mathbf{r}(\mathbf{v}, \mathbf{x}; t)\ _2$	$\Phi \hat{\mathbf{x}}^n = \operatorname{argmin}_{\mathbf{v} \in \operatorname{range}(\Phi)} \ \mathbf{r}^n(\mathbf{v})\ _2$

- C., Choi, and Sargsyan. “Conservative model reduction for finite-volume models.” J Comp Phys, 371:280–314, 2018.
- Lee and C. “Deep conservation: A latent dynamics model for exact satisfaction of physical conservation laws.” arXiv e-print 1909.09754, 2019.

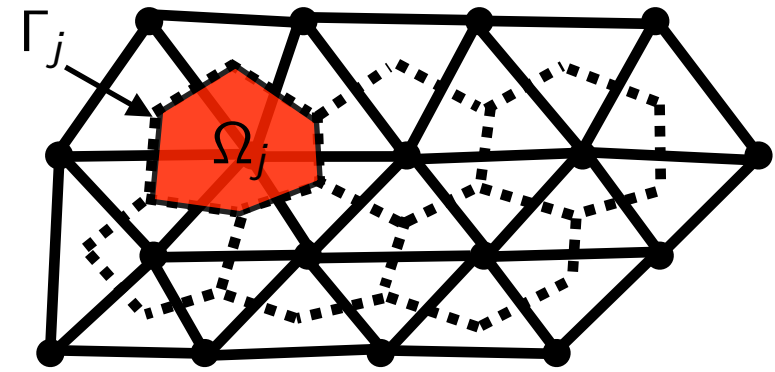
## 3) Error analysis difficult

- Freno and C. “Machine-learning error models for approximate solutions to parameterized systems of nonlinear equations.” CMAME, 348:250–296, 2019.
- Parish and C. “Time-series machine-learning error models for approximate solutions to parameterized dynamical systems.” arXiv e-print, (1907.11822).



# Finite-volume method

$$\text{ODE: } \frac{d\mathbf{x}}{dt} = \mathbf{f}(\mathbf{x}; t)$$



$$x_{\mathcal{I}(i,j)}(t) = \frac{1}{|\Omega_j|} \int_{\Omega_j} u_i(\vec{x}, t) d\vec{x}$$

- average value of conserved variable  $i$  over control volume  $j$

$$f_{\mathcal{I}(i,j)}(\mathbf{x}, t) = -\frac{1}{|\Omega_j|} \int_{\Gamma_j} \underbrace{\mathbf{g}_i(\mathbf{x}; \vec{x}, t) \cdot \mathbf{n}_j(\vec{x})}_{\text{flux}} d\vec{s}(\vec{x}) + \frac{1}{|\Omega_j|} \int_{\Omega_j} \underbrace{s_i(\mathbf{x}; \vec{x}, t)}_{\text{source}} d\vec{x}$$

- flux and source of conserved variable  $i$  within control volume  $j$

$$r_{\mathcal{I}(i,j)} = \frac{dx_{\mathcal{I}(i,j)}}{dt}(t) - f_{\mathcal{I}(i,j)}(\mathbf{x}, t)$$

- rate of conservation violation of variable  $i$  in control volume  $j$

$$\text{ODE: } \mathbf{r}^n(\mathbf{x}^n) = 0, \quad n = 1, \dots, N$$

$$r_{\mathcal{I}(i,j)}^n = x_{\mathcal{I}(i,j)}(t^{n+1}) - x_{\mathcal{I}(i,j)}(t^n) + \int_{t^n}^{t^{n+1}} f_{\mathcal{I}(i,j)}(\mathbf{x}, t) dt$$

- conservation violation of variable  $i$  in control volume  $j$  over time step  $n$

**Conservation is the intrinsic structure enforced by finite-volume methods**



# Conservative manifold model reduction

## Manifold Galerkin

$$\underset{\hat{\mathbf{v}} \in \mathbb{R}^p}{\text{minimize}} \|\mathbf{r}(\nabla \mathbf{g}(\hat{\mathbf{x}})\hat{\mathbf{v}}; \mathbf{g}(\hat{\mathbf{x}}); \mathbf{t})\|_2$$

- Minimize conservation-violation rates

## Manifold LSPG

$$\hat{\mathbf{x}}^n = \underset{\hat{\mathbf{v}} \in \mathbb{R}^p}{\text{argmin}} \|\mathbf{r}^n(\mathbf{g}(\hat{\mathbf{v}}))\|_2$$

- Minimize conservation violations over time step  $n$

- Neither enforces conservation!

## Conservative manifold Galerkin

$$\underset{\hat{\mathbf{v}} \in \mathbb{R}^p}{\text{minimize}} \|\mathbf{r}(\nabla \mathbf{g}(\hat{\mathbf{x}})\hat{\mathbf{v}}; \mathbf{g}(\hat{\mathbf{x}}); \mathbf{t})\|_2$$

subject to  $\mathbf{C}\mathbf{r}(\nabla \mathbf{g}(\hat{\mathbf{x}})\hat{\mathbf{v}}; \mathbf{g}(\hat{\mathbf{x}}); \mathbf{t}) = \mathbf{0}$

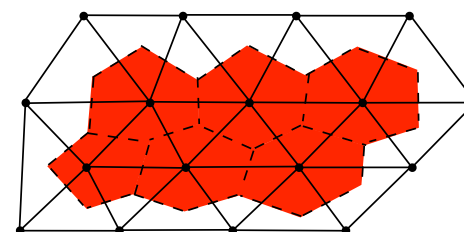
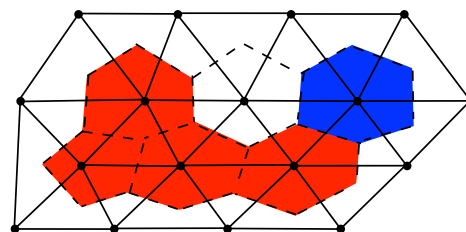
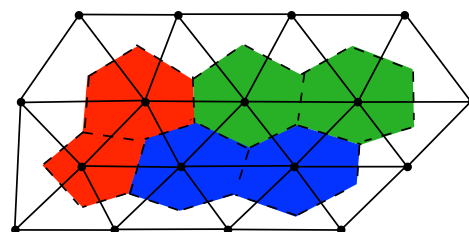
- Minimize conservation-violation rates  
subject to zero conservation-violation rates  
over subdomains

## Conservative manifold LSPG

$$\underset{\hat{\mathbf{v}} \in \mathbb{R}^p}{\text{minimize}} \|\mathbf{r}^n(\mathbf{g}(\hat{\mathbf{v}}))\|_2$$

subject to  $\mathbf{C}\mathbf{r}^n(\mathbf{g}(\hat{\mathbf{v}})) = \mathbf{0}$

- Minimize conservation violations over time step  $n$  subject to zero conservation violations over time step  $n$  over subdomains



+ Conservation enforced over prescribed subdomains

# Discrete-time error bound (linear subspaces)

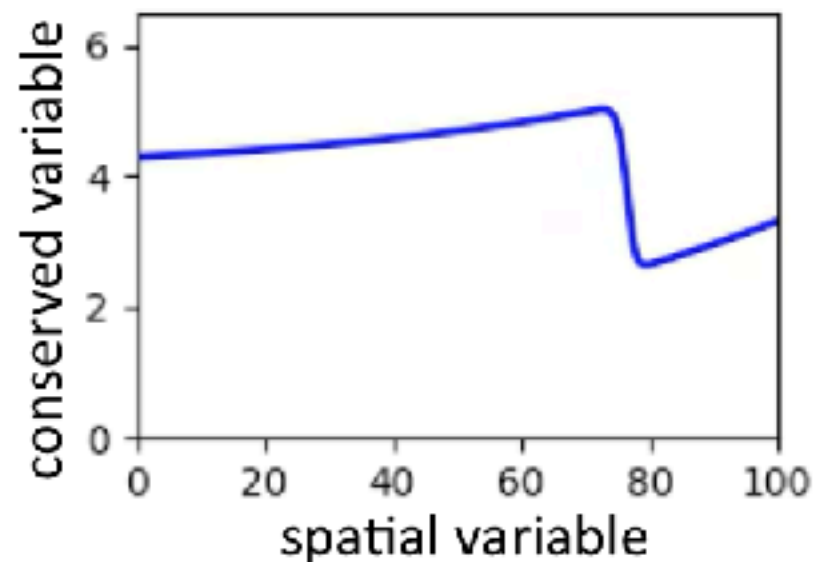
**Lemma:** local conserved-quantity error bounds [C., Choi, Sargsyan, 2018]

The error in the conserved quantities computed with either conservative Galerkin or conservative LSPG can be bounded as:

$$\begin{aligned} \|\bar{\mathbf{C}}(\mathbf{x}^n - \Phi \hat{\mathbf{x}}^n)\|_2 &\leq \sum_{\ell=0}^k \frac{|\beta_{\ell}^n| \Delta t}{|\alpha_0^n|} \|\bar{\mathbf{C}}\mathbf{f}(\mathbf{x}^{n-\ell}) - \bar{\mathbf{C}}\mathbf{f}(\Phi \hat{\mathbf{x}}^{n-\ell})\|_2 \\ &\quad + \sum_{\ell=1}^k \frac{|\alpha_{\ell}^n|}{|\alpha_0^n|} \|\bar{\mathbf{C}}(\mathbf{x}^{n-\ell} - \Phi \hat{\mathbf{x}}^{n-\ell})\|_2 \end{aligned}$$

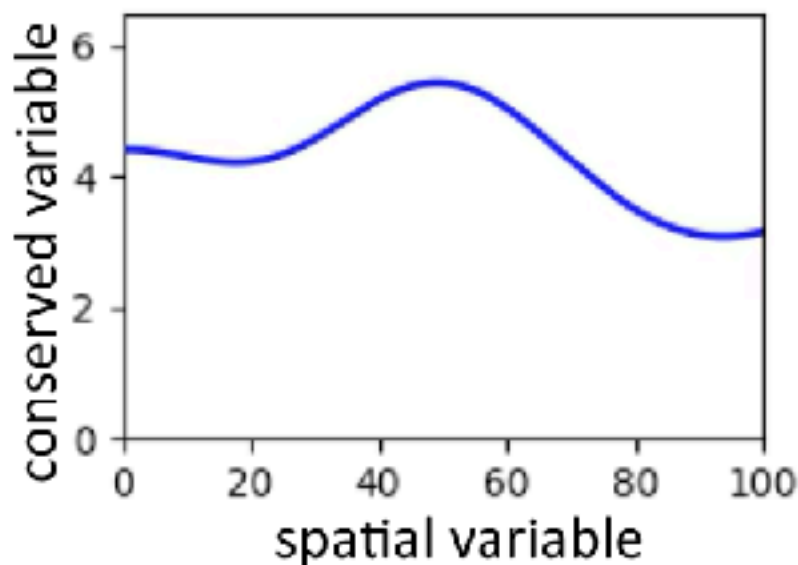
- Error depends only on velocity error on *decomposed mesh*
- + No source, global conservation: error due to **flux error along boundary!**

# High-fidelity model



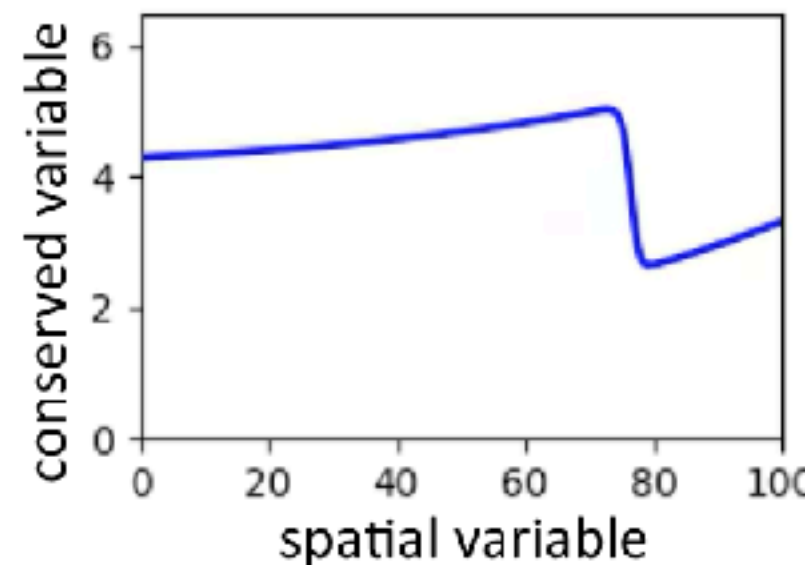
# Reduced-order models

## POD subspace



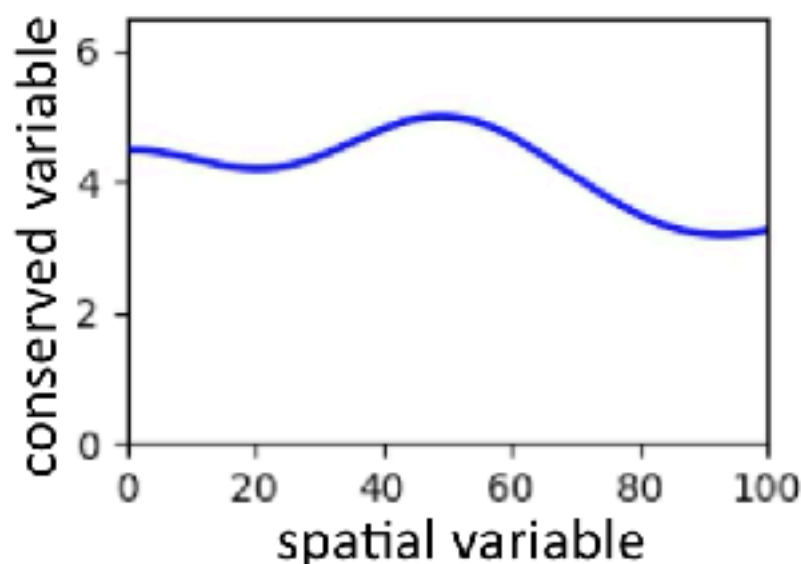
Solution error: **13%**  
Conservation violation: **16%**

## Autoencoder manifold



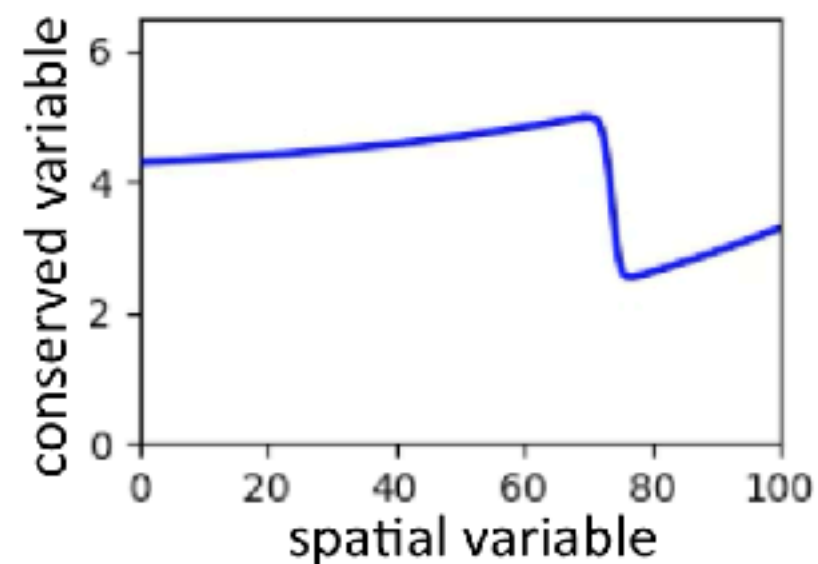
Solution error: **0.5%**  
Conservation violation: **1%**

## POD subspace with conservation constraints



Solution error: **12%**  
Conservation violation: **<0.001%**

## Autoencoder manifold with conservation constraints



Solution error: **0.2%**  
Conservation violation: **<0.001%**

# Outlook

## Conservative manifold Galerkin

$$\underset{\hat{\mathbf{v}} \in \mathbb{R}^p}{\text{minimize}} \|\mathbf{r}(\nabla \mathbf{g}(\hat{\mathbf{x}})\hat{\mathbf{v}}; \mathbf{g}(\hat{\mathbf{x}}); t)\|_2$$

$$\text{subject to } \mathbf{C}\mathbf{r}(\nabla \mathbf{g}(\hat{\mathbf{x}})\hat{\mathbf{v}}; \mathbf{g}(\hat{\mathbf{x}}); t) = \mathbf{0}$$

## Conservative manifold LSPG

$$\underset{\hat{\mathbf{v}} \in \mathbb{R}^p}{\text{minimize}} \|\mathbf{r}^n(\mathbf{g}(\hat{\mathbf{v}}))\|_2$$

$$\text{subject to } \mathbf{C}\mathbf{r}^n(\mathbf{g}(\hat{\mathbf{v}})) = \mathbf{0}$$

## Interpretation

- Integrates **computational physics** with **deep learning**
- *Projection-based latent dynamics model* that enforces conservation
- Nearly all existing methods are *data-driven latent dynamics models*

[Böhmer et al., 2015; Goroshin et al., 2015; Watter et al., 2015; Karl et al., 2017; Takeishi et al., 2017; Banijamali et al., 2018; Lesort et al., 2018; Lusch et al., 2018; Morton et al., 2018 Otto and Rowley, 2019]

## Gradient computation

- Backpropagation used to compute decoder Jacobian  $\nabla \mathbf{g}(\hat{\mathbf{x}})$
- Quasi-Newton solvers directly call TensorFlow

## Ongoing work

- *Hyper-reduction*: “easy” because convolutional layers preserve sparsity
- Integration in large-scale code underway in Pressio

# Shortcomings of state-of-the-art ROMs

## 1) Linear-subspace assumption is strong

$$\mathbf{x}(t) \approx \tilde{\mathbf{x}}(t) = \Phi \hat{\mathbf{x}}(t)$$

- Lee and C. “Model reduction of dynamical systems on nonlinear manifolds using deep convolutional autoencoders.” J Comp Phys, 404:108973, 2020.

## 2) Important physical properties not guaranteed

$$\Phi \frac{d\hat{\mathbf{x}}}{dt}(\mathbf{x}, t) = \underset{\mathbf{v} \in \text{range}(\Phi)}{\text{argmin}} \|\mathbf{r}(\mathbf{v}, \mathbf{x}; t)\|_2$$

*Galerkin*

$$\Phi \hat{\mathbf{x}}^n = \underset{\mathbf{v} \in \text{range}(\Phi)}{\text{argmin}} \|\mathbf{r}^n(\mathbf{v})\|_2$$

*LSPG*

- C., Choi, and Sargsyan. “Conservative model reduction for finite-volume models.” J Comp Phys, 371:280–314, 2018.
- Lee and C. “Deep conservation: A latent dynamics model for exact satisfaction of physical conservation laws.” arXiv e-print 1909.09754, 2019.

## 3) Error analysis difficult

- Freno and C. “Machine-learning error models for approximate solutions to parameterized systems of nonlinear equations.” CMAME, 348:250–296, 2019.
- Parish and C. “Time-series machine-learning error models for approximate solutions to parameterized dynamical systems.” arXiv e-print, (1907.11822).

# Discrete-time error bound

**Theorem:** error bound for BDF integrators [C., Barone, Antil, 2017]

If the following conditions hold:

1.  $\mathbf{f}(\cdot; t)$  is Lipschitz continuous with Lipschitz constant  $\kappa$
2. The time step  $\Delta t$  is small enough such that  $0 < h := |\alpha_0| - |\beta_0|\kappa\Delta t$ ,

$$\|\mathbf{x}^n - \mathbf{g}(\hat{\mathbf{x}}_G^n)\|_2 \leq \frac{1}{h} \|\mathbf{r}_G^n(\mathbf{g}(\hat{\mathbf{x}}_G))\|_2 + \frac{1}{h} \sum_{\ell=1}^k |\gamma_\ell| \|\mathbf{x}^{n-\ell} - \mathbf{g}(\hat{\mathbf{x}}_G)\|_2$$

$$\|\mathbf{x}^n - \mathbf{g}(\hat{\mathbf{x}}_{\text{LSPG}}^n)\|_2 \leq \frac{1}{h} \min_{\hat{\mathbf{v}}} \|\mathbf{r}_{\text{LSPG}}^n(\mathbf{g}(\hat{\mathbf{v}}))\|_2 + \frac{1}{h} \sum_{\ell=1}^k |\gamma_\ell| \|\mathbf{x}^{n-\ell} - \mathbf{g}(\hat{\mathbf{x}}_{\text{LSPG}})\|_2$$

***Can we use these error bounds for error estimation?***

# Discrete-time error bound

**Theorem:** error bound for BDF integrators [C., Barone, Antil, 2017]

If the following conditions hold:

1.  $\mathbf{f}(\cdot; t)$  is Lipschitz continuous with Lipschitz constant  $\kappa$
2. The time step  $\Delta t$  is small enough such that  $0 < h := |\alpha_0| - |\beta_0|\kappa\Delta t$ ,

$$\|\mathbf{x}^n - \mathbf{g}(\hat{\mathbf{x}}_G^n)\|_2 \leq \frac{\gamma_1(\gamma_2)^n \exp(\gamma_3 t^n)}{\gamma_4 + \gamma_5 \Delta t} \max_{j \in \{1, \dots, N\}} \|\mathbf{r}_{\text{LSPG}}^j(\mathbf{g}(\hat{\mathbf{x}}_G^j))\|_2$$

$$\|\mathbf{x}^n - \mathbf{g}(\hat{\mathbf{x}}_{\text{LSPG}}^n)\|_2 \leq \frac{\gamma_1(\gamma_2)^n \exp(\gamma_3 t^n)}{\gamma_4 + \gamma_5 \Delta t} \max_{j \in \{1, \dots, N\}} \min_{\hat{\mathbf{v}}} \|\mathbf{r}_{\text{LSPG}}^j(\mathbf{g}(\hat{\mathbf{v}}))\|_2$$

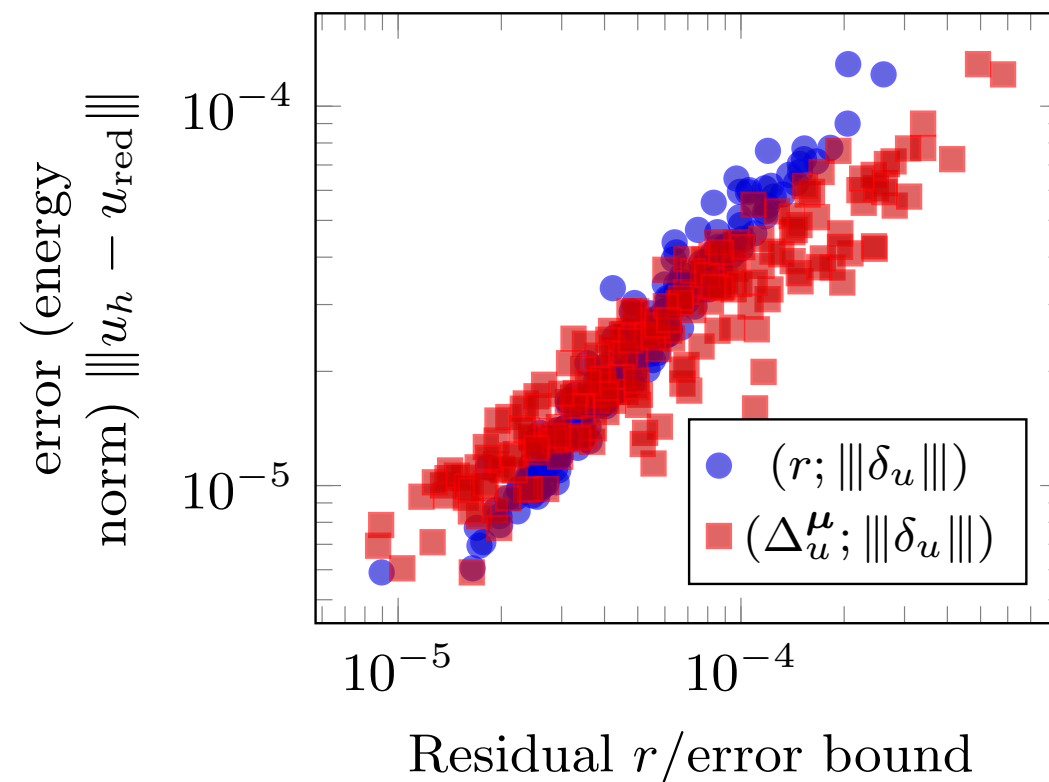
***Can we use these error bounds for error estimation?***

- grow exponentially in time
- deterministic: not amenable to uncertainty quantification



# Main idea

- **Observation:** ROMs generate quantities that are **informative** of the error



- **ML perspective:** these are **good features** for predicting the error

*Idea: Apply machine learning regression to generate a mapping from residual-based quantities to a random variable for the error*

**Machine-learning error models** [Freno and C., 2019; Parish and C., 2019]



# Machine-learning error models: formulation

*What attributes does the ROM error have?*

$$\|\mathbf{x}^n - \mathbf{g}(\hat{\mathbf{x}}_{\text{LSPG}}^n)\|_2 \leq \frac{\gamma_1 (\gamma_2)^n \exp(\gamma_3 t^n)}{\gamma_4 + \gamma_5 \Delta t} \max_{j \in \{1, \dots, T\}} \min_{\hat{\mathbf{v}}} \|\mathbf{r}_{\text{LSPG}}^j(\mathbf{g}(\hat{\mathbf{v}}))\|_2$$

1. Dependence on non-local quantities in time
2. Dependence on the residual

*Regression model*

$$\hat{\delta}^n(\boldsymbol{\mu}) = \underbrace{\hat{\delta}_f^n(\boldsymbol{\mu})}_{\text{deterministic}} + \underbrace{\hat{\delta}_\epsilon^n(\boldsymbol{\mu})}_{\text{stochastic}}$$

▸ regression function:  $\hat{\delta}_f^n(\boldsymbol{\mu}) = \hat{f}(\boldsymbol{\rho}^n(\boldsymbol{\mu}), \mathbf{h}^{n-1}(\boldsymbol{\mu}), \hat{\delta}_f^{n-1}(\boldsymbol{\mu}))$

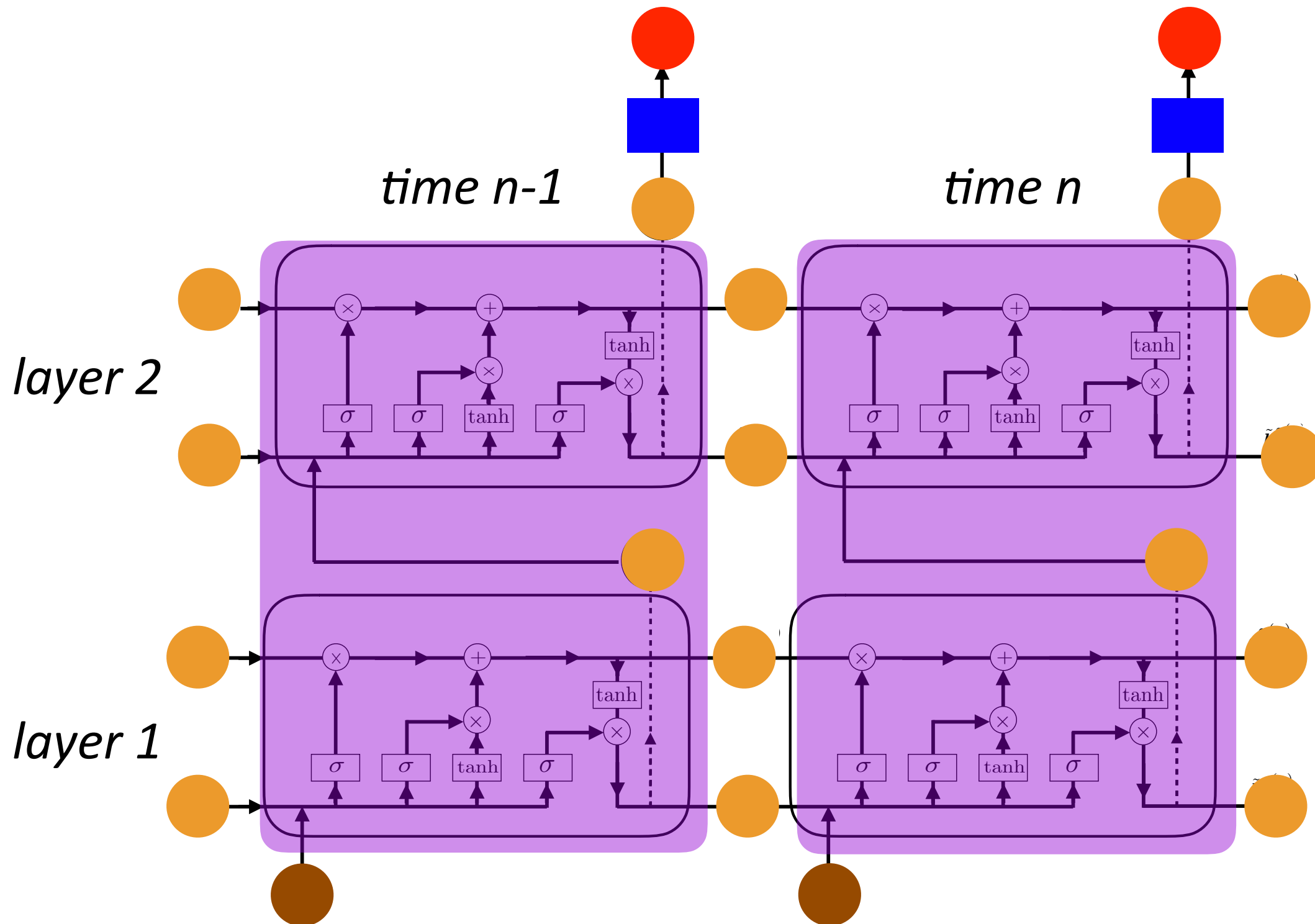
$$\mathbf{h}^n(\boldsymbol{\mu}) = \mathbf{g}(\boldsymbol{\rho}^n(\boldsymbol{\mu}), \mathbf{h}^{n-1}(\boldsymbol{\mu}), \hat{\delta}_f^{n-1}(\boldsymbol{\mu}))$$

- + latent variables  $\mathbf{h}^n(\boldsymbol{\mu})$ : enable capturing non-local dependencies
- + features  $\boldsymbol{\rho}^n(\boldsymbol{\mu})$ : residual-based (and cheaply computable)
- + general formulation encompasses ARX, LARX, RNN, LSTM, GRU

# Example: long short-term memory (LSTM)

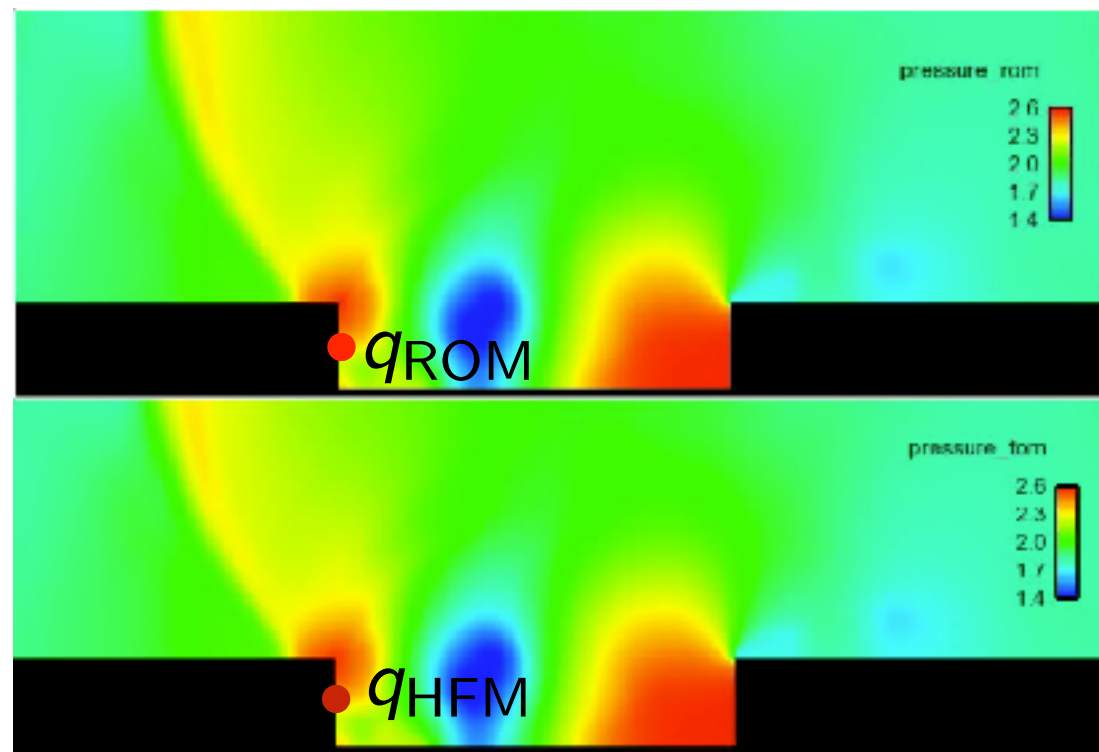
$$\hat{\delta}_f^n(\mu) = \hat{f}(\rho^n(\mu), h^{n-1}(\mu))$$

$$h^n(\mu) = g(\rho^n(\mu), h^{n-1}(\mu))$$

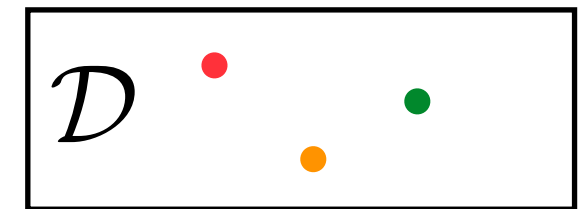


# Training and machine learning: error modeling

1. *Training*: Solve high-fidelity and reduced-order models for  $\mu \in \mathcal{D}_{\text{training}}$
2. *Machine learning*: Construct regression model
3. *Reduction*: predict reduced-order-model error for  $\mu \in \mathcal{D}_{\text{query}} \setminus \mathcal{D}_{\text{training}}$



$$q_{\text{HFM}}^n - q_{\text{ROM}}^n$$



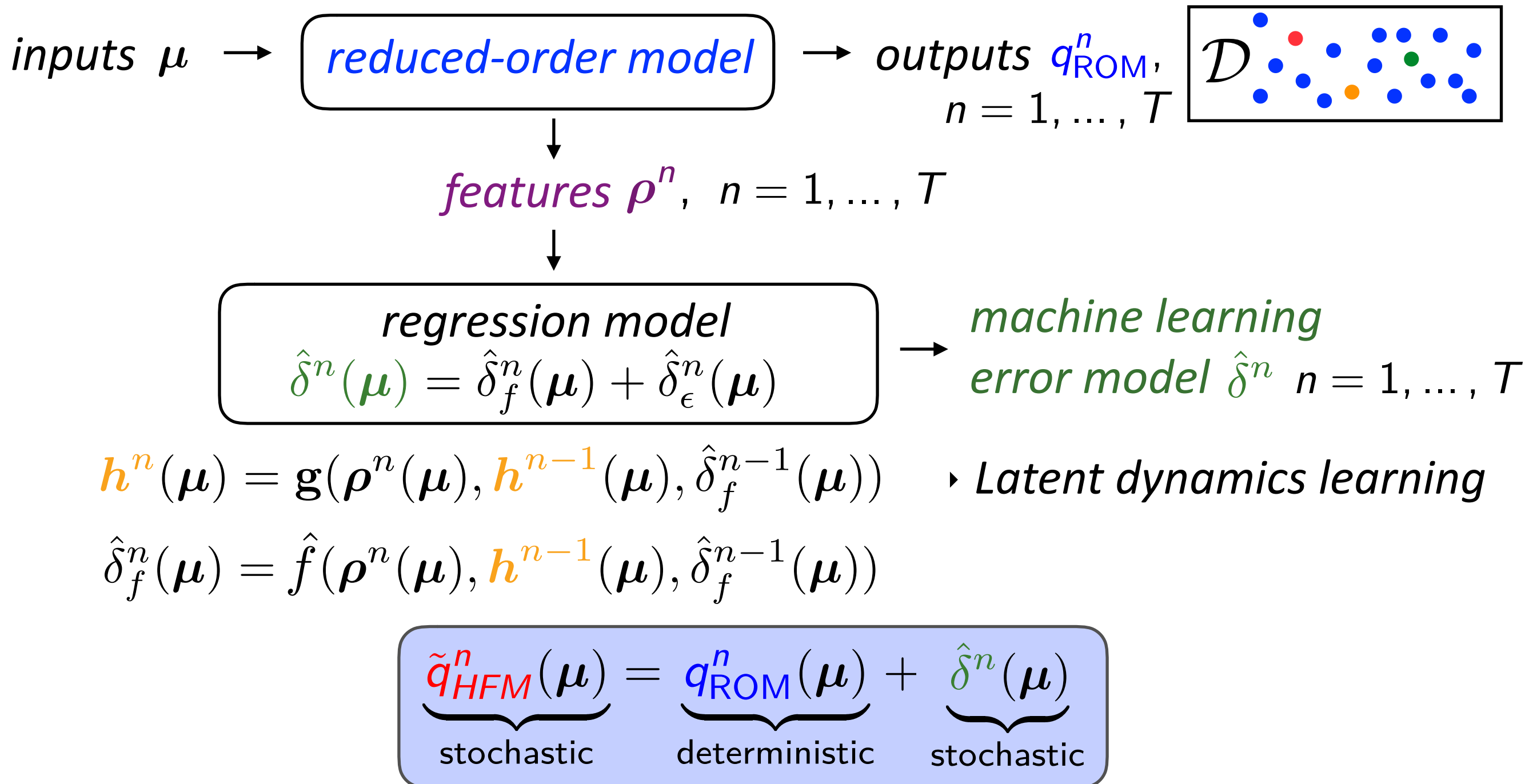
$$\rho^n$$



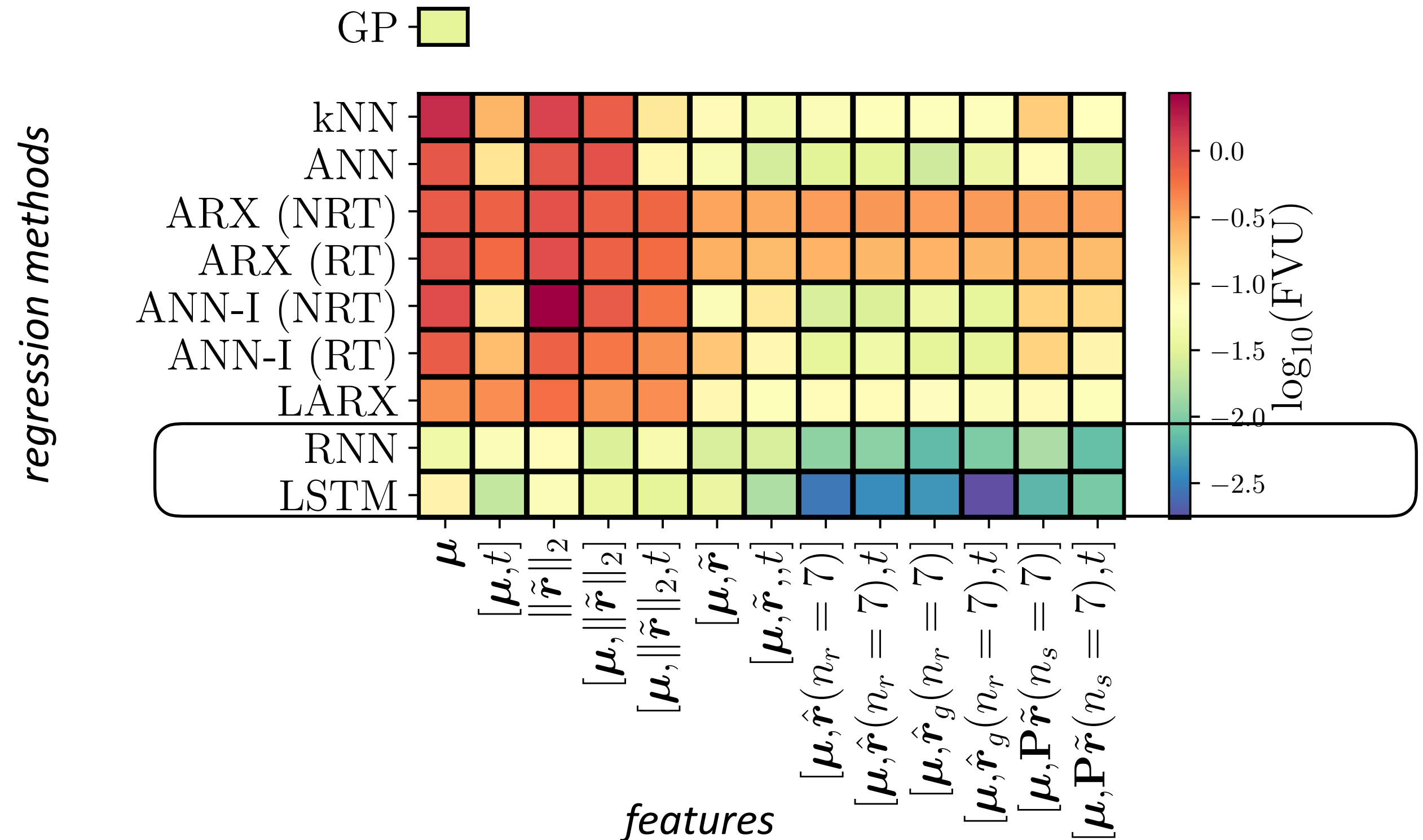
- randomly divide data into (1) training data and (2) testing data
- construct regression function  $\hat{\delta}_f^n$  via cross validation on **training data**
- construct noise model  $\hat{\delta}_\epsilon^n$  from sample variance on **test data**

# Reduction

1. *Training*: Solve high-fidelity and reduced-order models for  $\mu \in \mathcal{D}_{\text{training}}$
2. *Machine learning*: Construct regression model
3. *Reduction*: predict reduced-order-model error for  $\mu \in \mathcal{D}_{\text{query}} \setminus \mathcal{D}_{\text{training}}$

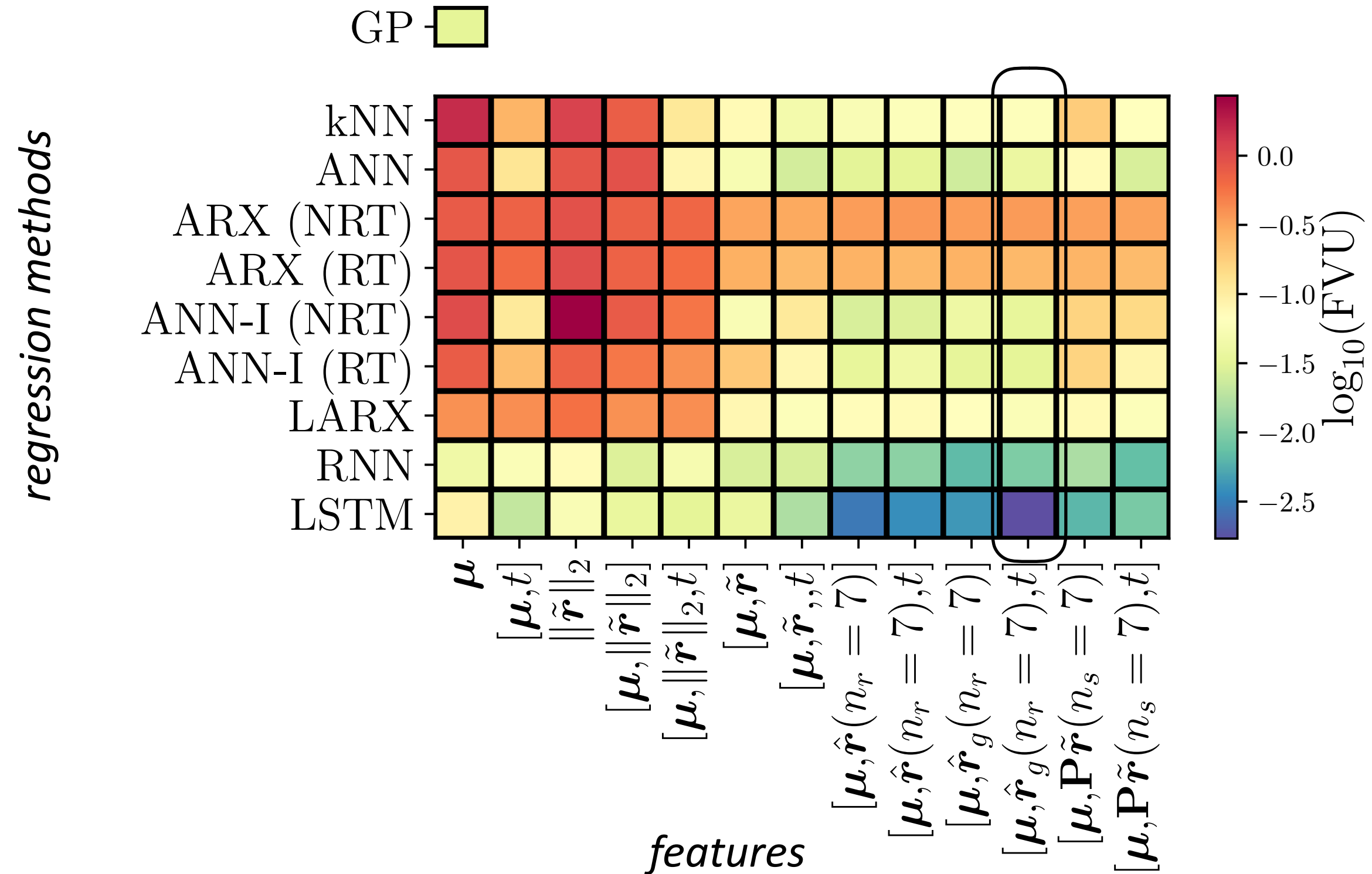


# Application: Advection–diffusion equation



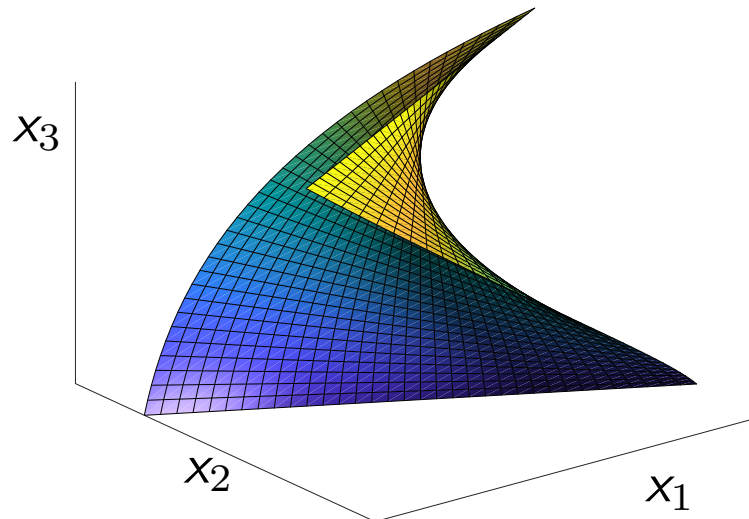
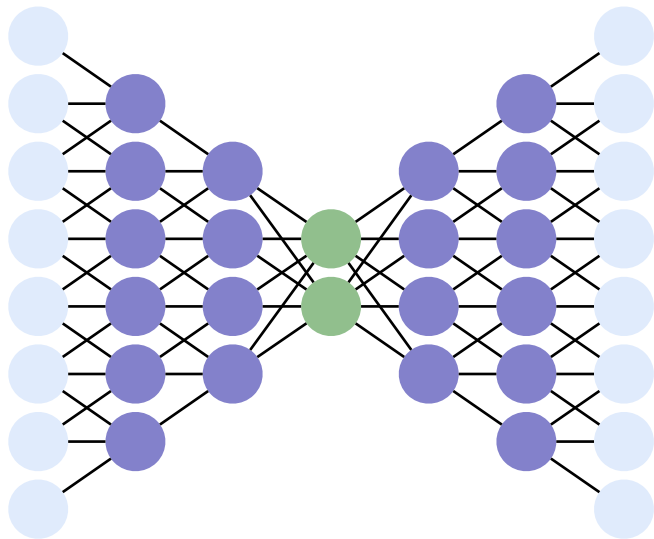
+ regression methods: classical RNN and LSTM **most accurate**

# Application: Advection–diffusion equation

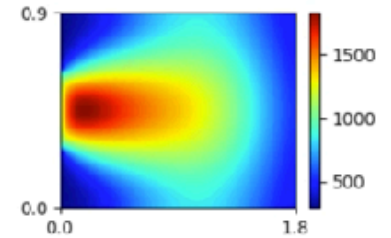


- + *regression methods*: classical RNN and LSTM **most accurate**
- + *features*: only 7 residual samples needed for **good accuracy**

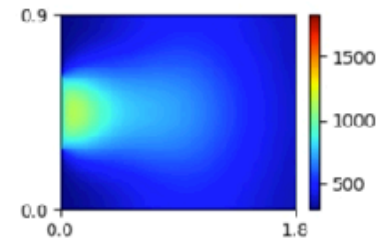
# Questions?



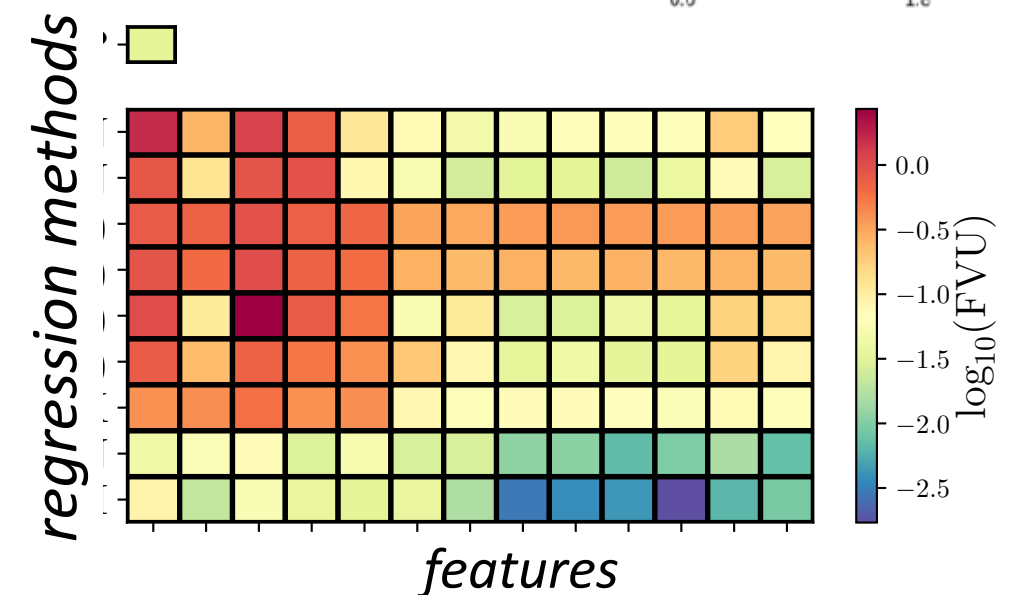
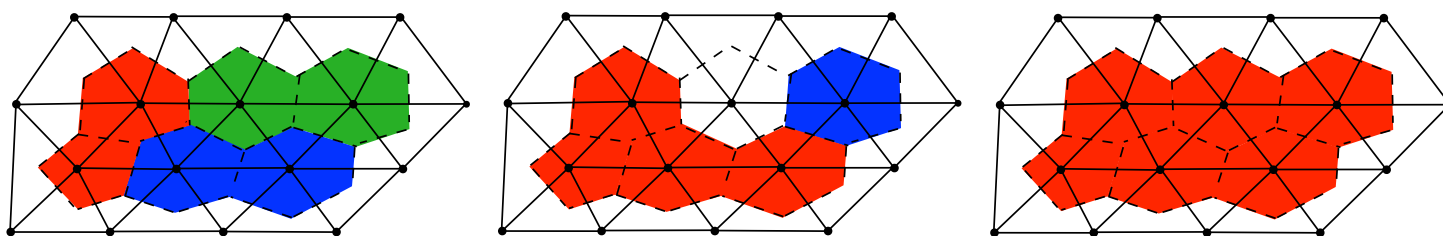
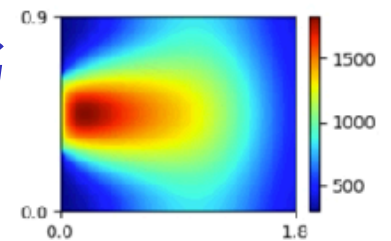
high-fidelity  
model



POD-LSPG  
 $p=5$



Manifold LSPG  
 $p=5$



Sandia National Laboratories is a multimission laboratory managed and operated by National Technology and Engineering Solutions of Sandia, LLC., a wholly owned subsidiary of Honeywell International, Inc., for the U.S. Department of Energy's National Nuclear Security Administration under contract DE-NA-0003525. Lawrence Livermore National Laboratory is operated by Lawrence Livermore National Security, LLC, for the U.S. Department of Energy, National Nuclear Security Administration under Contract DE-AC52-07NA27344.